

1 Dear Referee,

2 Thank you very much for your valuable suggestions and comments. We have tried to implement  
3 each point by point. Please see the blue coloured text is answers to the query. Detailed explanations  
4 with updated figures have been incorporated in the revised manuscript.

5 **Referee#1:**

6 General comments: Atmospheric greenhouse gases (GHGs) are important climate forcing agents  
7 and have significant impacts on global climate. This study brings out first continuous  
8 measurements of atmospheric GHGs (CO<sub>2</sub> and CH<sub>4</sub>) using high precision Los Gatos Research's  
9 greenhouse gas analyser (LGR-GGA) over Shadnagar, a suburban site of Central India during the  
10 period of 2014. The authors also investigate the influences of meteorology on GHGs and their  
11 interrelationship. It is useful to estimate quantitatively the radiative effects of GHGs on regional  
12 or global climate change. Obviously, there are numerous grammatical and technical errors in the  
13 manuscript. This paper is reconsidered to be acceptable and published after major revisions.

14 Specific comments:

15 Q1). Abstract, lines 1-18: "Atmospheric greenhouse gases (GHGs) such as carbon dioxide: : : :  
16 :It implies the seasonal variations in source-sink mechanisms of CO<sub>2</sub> and CH<sub>4</sub>. Present study also  
17 confirms implicitly the presence OH radicals as a major sink of CH<sub>4</sub> over the study region".  
18 This study aims to analyse the seasonal variations of CO<sub>2</sub> and CH<sub>4</sub> over a suburban site of Central  
19 India and investigate the influences of prevailing meteorology (e.g., air temperature, wind speed,  
20 wind direction, relative humidity, boundary layer height) on GHGs and their interrelationship. The  
21 manuscript also reveals that biomass burning (forest fire and crop residue burning) has a role in  
22 pre-monsoon enhancement of CO<sub>2</sub> over study site (Page 34219, lines 4-17). And the air mass  
23 trajectories of crops agriculture residue burning in the NW and NE regions part of India can reach  
24 the study site at different altitudes during post-monsoon to early pre-monsoon (Page 34220, lines  
25 1-5). Therefore, in order to investigate the exact influences of prevailing meteorology on GHGs,  
26 the CO<sub>2</sub> contributions of regional biomass burning and long range transport should be excluded  
27 from the CO<sub>2</sub> measurements. Otherwise, many conclusions in present study make no sense.

28 Answer: We agree with referee suggestions. Inorder to investigate the exact influences of  
29 prevailing meteorology on GHGs, we have done the analysis, by eleminating those study days  
30 where biomass burnig influence are there. Biomass burning days are identified using MODIS  
31 active fire count data during the study period. Figure 3a-c is updated accordingly.

32 Q2). "4.6 Influence of vegetation on GHGs", Page34218, lines 25-28 and Page34219, lines 1-3:  
33 "The main source for CH<sub>4</sub> emissions are soil microbial (Kirschke et al., 2013) activity which are  
34 more active during monsoon and post monsoon seasons: : : :The predominating factors which  
35 control the soil emissions of CO<sub>2</sub> and CH<sub>4</sub> are moisture content, soil temperature, vegetation and  
36 soil respiration (Smith et al., 2003; Jones et al., 2005; Chen et al., 2010) respectively." So,  
37 we recommend strongly that the authors add and discuss the possible influences of soil parameters  
38 (such as, moisture content, soil temperature, vegetation and soil respiration) on GHGs and their  
39 interrelationship in the manuscript. And we believe that the authors would acquire many  
40 interesting findings.

Answer: As per referee suggestion we have studied the influence of soil moisture and temperature on GHGs. A new figure (Figure 8) is added illustrating the influence of soil moisture and temperature on GHGs and corresponding discussion are provided in the manuscript.

Q3). Page 34212, lines 6-9: "Enhancement in pre-monsoon is due to higher temperature and solar radiation prevailing during these months which stimulate the assimilation of CO<sub>2</sub> in the daytime and respiration in the night (Fang et al., 2014)" As discussing in the later section (4.6 and 4.7), quantitative contributions of regional biomass burning and long range transport to atmospheric CO<sub>2</sub> concentration at the study site are very important to the interpretation of enhancement CO<sub>2</sub> in pre-monsoon.

Answer: A quantative analysis (in terms of a case study) of regional/long range transported influence of biomass burning on local GHGs concencetration is provided in section 4.2.

Q4). Figure 3 to Figure 5: The authors study the interrelationships between monthly mean meteorology and GHGs. We suggest that the authors add the interrelationships between daily mean meteorology and GHGs, whether it is the same variation with monthly mean? If not, what is about for daily average?

Answer: Figure 3 and 4 updated as figure 6 to figure 8 and figure 5 as figure 9 in the revised manuscript. In figure 6-8, interrelationships are analysed using daily mean data. Each points in the Figure 6-8 represent daily mean corresponding to each season. However for Figure 9 (Seasonal variation of GHGs and Boundary layer height) daily data on boundary layer height over study region is not available from satellite, we used ECMWF-ERA data to study the diurnal boundary layer (figure 5) effect on GHGs mixing ratios over study region.

Minor Comments:

Comment: 1

Title: "Influence of meteorology and interrelationship with greenhouse gases (CO<sub>2</sub> and CH<sub>4</sub>) at a sub-urban site of India" Change "sub-urban" to "suburban", and modify the other places in the whole manuscript.

Answer: The correction is incorporated in the revised manuscript.

Comment: 2

Abstract, Page 34206, lines 2-4: "Atmospheric greenhouse (GHGs) such as carbon dioxide (CO<sub>2</sub>) and methane (CH<sub>4</sub>) are important climate forcing agents due to their significant impact on the climate system." Change to "Atmospheric greenhouse (GHGs), such as carbon dioxide (CO<sub>2</sub>) and methane (CH<sub>4</sub>), are important climate forcing agents due to their significant impacts on the climate system."

Answer: The correction is incorporated in the revised manuscript

Comment: 3

84 Abstract, Page 34206, line 5; Page 34207, line 24; Page 34208, line 7: change “GHG’s” to  
85 “GHGs”, and modify the other places in the whole manuscript.

86

87 [Answer: updated in the revised manuscript](#)

88

89 Comment: 4

90 Abstract, Page 34206, lines 6-8; Page 34220, lines 10-11: “The annual mean of CO<sub>2</sub> and CH<sub>4</sub> over  
91 the study region is found to be 394\_2.92 and 1.92\_0.07 ppm (mean,  $\bar{A}_i \pm 1SD, \bar{A}_{i,s}$ ) respectively.”  
92  $\hat{A}_i \pm \hat{S}$  Change to “The annual mean CO<sub>2</sub> and CH<sub>4</sub> over the study region are found to be 394\_2.92  
93 ppm and 1.92\_0.07 ppm (mean\_standard deviation,  $\bar{A}_i \pm \bar{A}_{i,s}$ ) respectively.”

94

95 [Answer: The correction is incorporated in the revised manuscript.](#)

96

97 Comment: 5

98

99 Abstract, Page 34206, line 8, line 14; Page 34220, line 11: change “showed” to “show” and keep  
100 the consistency in the manuscript.

101

102 [Answer: Corrected as suggested.](#)

103

104 Comment: 6

105

106 Abstract, Page 34206, lines 14-16: “CO<sub>2</sub> and CH<sub>4</sub> showed a strong positive correlation during  
107 winter, pre-monsoon, monsoon and post-monsoon with R equal to 0.80, 0.80, 0.61 and 0.72  
108 respectively.”  $\hat{A}_i \pm \hat{S}$  Change to “CO<sub>2</sub> and CH<sub>4</sub> show a strong positive correlation during winter,  
109 pre-monsoon, monsoon, and post-monsoon with correlation coefficients (Rs) equal to 0.80, 0.80,  
110 0.61, and 0.72, respectively.”

111

112 [Answer: The correction is incorporated in the revised manuscript.](#)

113

114 Comment: 7

115 “Abstract, Page 34206, lines 17-18: “Present study also confirms implicitly the presence OH  
116 radicals as a major sink of CH<sub>4</sub> over the study region.”  $\hat{A}_i \pm \hat{S}$  Change to “Present study also  
117 confirms implicitly the presence hydroxyl radicals (OH) as a major sink of CH<sub>4</sub> over the study  
118 region.”

119

120 [Answer: Updated in the revised manuscript.](#)

121

122 Comment: 8

123 Page 34206, line 21: change “globalwaming” to “global warming”

124 [Answer: Updated in the revised manuscript.](#)

125

126 Comment: 9

127 Page 34206, lines 22-24: “CO<sub>2</sub> and CH<sub>4</sub> concentrations have increased by 40 and 150âG~ Š Change to  
128 “CO<sub>2</sub> and CH<sub>4</sub> concentrations have increased by 40 Please add the citation of Huang et al., 2015 in the  
129 manuscript: Huang J.\*, Yu H., Guan X., Wang G. and Guo R., 2015: Accelerated dryland expansion under  
130 climate change, Nature Climate Change, doi:10.1038/nclimate2837.

131  
132 Answer: Thanks to reviewer for providing very useful information and suggestions about the  
133 GHGs variability of arid and semiarid areas. It helped to improve the manuscript. We have  
134 included Huang et. al (2015) reference in the manuscript.

135  
136 Reference: Huang, J., Yu, H., Guan, X., Wang, G., & Guo, R. (2015). Accelerated dryland  
137 expansion under climate change. Nature Climate Change, doi:10.1038/nclimate2837.

138  
139  
140  
141 Comment: 10

142 Page 34207, line 3: change “constitutes” to “constitute”

143 Answer: Updated in the revised manuscript.

144  
145 Comment: 11, 12, 13, and 14

146 Page 34207, line 6: delete “that” (12) Page 34207, line 8: change “andecosystems” to “and ecosystems”  
147 (13) Page 34207, line 13: change “the part of the atmosphere” to “part of the atmosphere” (14) Page 34207,  
148 line 14: change “donimatethe” to “dominate the”

149  
150 Answer: Updated in the revised manuscript.

151  
152 Comment: 15

153 Page 34208, lines 5-7: “Major source of pollutants over Shadnagar can be from small and medium  
154 scale industries, biomass burning and bio-fuel aswell as from domestic cooking.” âG~ Š Change  
155 to “Major sources of pollutants over Shadnagar can be from small and medium scale industries,  
156 biomass burning and bio-fuel as well as from domestic cooking.”

157  
158 Answer: Incorporated in the revised manuscript.

159  
160 Comment: 16

161 Page 34208, lines 11-12: “Mean monthly variations of temperature (â~D ~ C) and RH (â ~ GŠ  
162 Change to “Monthly mean variations of temperature (â~DC~ ) and relative humidity (RH,

163 Answer: Updated in the manuscript.

164  
165 Comment: 17

166 Page 34208, line 16: Change “Relative humidity (RH) in Shadnagar reached a maximum of 82

167 Answer: Updated in the manuscript.

168  
169 Comment: 18

170  
171 Page 34209, lines 17-21: “In the present study we used GGA retrieved CO<sub>2</sub> and CH<sub>4</sub> data. High  
172 resolution data are diurnally averaged and is used in further analysis. Due to failure of internal  
173 central processing unit (CPU) of the analyzer data is not recorded from pre-monsoon month of  
174 May to a few days in June during the study period.” âG~ Š Change to “In the present study we used  
175 GGA to retrieve CO<sub>2</sub> and CH<sub>4</sub> data. High resolution data sets are diurnally averaged and used in  
176 further analysis. Due to failure of internal central processing unit (CPU) of the analyzer, data are  
177 not recorded from pre-monsoon month of May to a few days in June during the study period.”  
178

179 [Answer: The correction is incorporated in the revised manuscript.](#)

180  
181 Comment: 19

182 Page 34209, lines 23-25: “Surface concentrations of O<sub>3</sub> and NO<sub>x</sub> have been measured  
183 continuously using on-line analyzers Model No.s: 49i and 42i for O<sub>3</sub> and NO<sub>x</sub> respectively,  
184 procured from Thermo Scientific, USA) since July 2014.” âG~ Š Change to “Surface  
185 concentrations of O<sub>3</sub> and NO<sub>x</sub> have been measured continuously using on-line analyzers (Model  
186 No.s: 49i and 42i for O<sub>3</sub> and NO<sub>x</sub> respectively), procured from Thermo Scientific, USA since  
187 July 2014.”  
188

189 [Answer: The brackets modified in the revised manuscript.](#)

190  
191 Comment: 20

192 Page 34210, lines 2-3: “The NO<sub>x</sub> analyzer utilizes a molybdenumconverter to convert NO<sub>2</sub> into  
193 NO and estimates the NO<sub>x</sub> concentration: : :” âG~ Š Change to “The NO<sub>x</sub> analyzer utilizes a  
194 molybdenum converter to convert NO<sub>2</sub> into NO and estimate the NO<sub>x</sub> concentration: : :”  
195

196 [Answer: Incorporated in the revised manuscript.](#)

197  
198 Comment: 21, 22, & 23

199 Page 34210, line 5: change “zero and span calibration” to “zero and span calibrations” (22) Page  
200 34210, line 7: change “an automatic weather stations (AWS)” to “an automatic weather station  
201 (AWS)” (23) Page 34210, line 13: change “of 250, 500 m, and 1 km” to “of 250 m, 500 m, and 1  
202 km”  
203

204 [Answer: Incorporated in the revised manuscript.](#)

205  
206 Comment: 24

207 Page 34211, lines 7-8: “Geophysical parameters like temperature and humidity profiles have been  
208 simultaneously obtained from: : :” âG~ Š Change to “Geophysical parameters (such as, temperature  
209 and humidity profiles) have been simultaneously obtained from: : :”  
210

211 [Answer: Updated in the revised manuscript.](#)

212  
213 Comment: 25 & 26

214 Page 34212, lines 1-2: “Background (average) values of CO<sub>2</sub>: : :” âG~ Š Please add “How to define  
215 or calculate background average values of CO<sub>2</sub>: : :” (26) Page 34212, line 3: change “and 392\_7.0  
216 and 393\_7.0 ppm with respectively winter, pre-monsoon, monsoon and post-monsoon.” to  
217 “392\_7.0, and 393\_7.0 ppm respectively with winter, pre-monsoon, monsoon, and post-monsoon.”

218

219 [Answer: The correction is incorporated in the revised manuscript.](#)

220

221 Comment: 27, 28, and 29

222 Page 34213, line 4: change “Figure 2c and d depicts” to “Figure 2c and 2d depict” (28) Page 34213,  
223 line 6: change “such as land use land cover change” to “such as land use and land cover change”  
224 (29) Page 34213, line 26: change “while a not so significant correlation suggest the influence of  
225 regional transport” to “while a not so significant correlation suggests the influence of regional  
226 transport”

227

228 [Answer: Updated in the manuscript.](#)

229

230 Comment: 30

231 Page 34214, lines 1-5: “Figure 3a and b shows scatter plot between GHG’s and wind speed during  
232 different seasons. Analysis of Fig. 3b shows that there exist an inverse correlation between  
233 monthly mean wind speed and GHG’s. Correlation coefficient (R) between wind speed and CO<sub>2</sub>  
234 during pre-monsoon, monsoon, post-monsoon and winter is 0.56, 0.32, 0.06 and 0.67  
235 respectively.” âG~ Š Change to “Figure 3a and 3b show scatter plot between GHG’s and wind  
236 speed during different seasons. Fig. 3b shows that there exists an inverse correlation between  
237 monthly mean wind speed and GHG. Correlation coefficients (Rs) between wind speed and CO<sub>2</sub>  
238 during pre-monsoon, monsoon, post-monsoon, and winter are 0.56, 0.32, 0.06, and 0.67,  
239 respectively.”

240

241 [Answer: Incorporated in the revised manuscript.](#)

242

243 Comment: 31, 32, 33, 35 and 36

244 Page 34214, line 16: change “The meteorological parameters (temperature and relative humidity)  
245 influenceon trace gases” to “The influence of meteorological parameters (temperature and relative  
246 humidity) on trace gases” (33) Page 34214, line 18: change “shows the scatter plot of temperature  
247 vs. relative humidity” to “show the scatter plot of temperature versus relative humidity” (34) Page  
248 34214, line 19: change “Hence, dailymean data” to “Hence, daily mean data” (35) Page 34215,  
249 line 17: change “An average monthly air temperature” to “A monthly average air temperature”

250

251 [Answer: Incorporated in the revised manuscript.](#)

252 Comment: 36

253

254 Page 34216, line 1: change “between hourly averaged CO<sub>2</sub> and CH<sub>4</sub> during all season” to “between  
255 hourly average CO<sub>2</sub> and CH<sub>4</sub> during all seasons”

256

257 [Answer: Updated in the revised manuscript.](#)

258  
259 Comment: 37  
260  
261 Page 34216, line 21: change “is” to “are”  
262  
263 Answer: [Changed as suggested.](#)  
264  
265 Comment: 38  
266  
267 Page 34217, lines 3-6: “Atmospheric CH<sub>4</sub> is mainly (70-80%) Hence, it is very essential to  
268 discuss the possible influences of soil parameters (such as, moisture content, soil temperature,  
269 vegetation and soil respiration) on GHGs and their interrelationship in the manuscript.  
270  
271 Answer: [We updated in the revised manuscript at section 4.5.](#)  
272  
273 Comment: 39  
274  
275 Page 34218, lines 20-21: change “..is calculated from daily day time (10:00-16:00 LT) mean.” to  
276 “..is calculated from daily mean in day time (10:00-16:00 LT).”  
277  
278 Answer: [Incorporated in the revised manuscript.](#)  
279  
280 Comment: 40  
281  
282 Page 34219, line 19: change “To understand the role of long range circulation we separated the  
283 trajectory into 4 clusters” to “To understand the role of long range circulation, we separated the  
284 trajectory into 4 clusters”  
285  
286 Answer: [Updated in the manuscript.](#)  
287  
288 Comment: 41  
289  
290 Page 34220, lines 20-22: “Correlation coefficient (R) between wind speed and CO<sub>2</sub> during pre-  
291 monsoon, monsoon, post-monsoon and winter is 0.56, 0.32, 0.06 and 0.67 respectively. While for  
292 CH<sub>4</sub> it is found to be 0.28, 0.71, 0.21, and 0.60 respectively.” Change to “Correlation  
293 coefficients (Rs) between wind speed and CO<sub>2</sub> during pre-monsoon, monsoon, post-monsoon and  
294 winter are 0.56, 0.32, 0.06, and 0.67, respectively. While CH<sub>4</sub> are found to be 0.28, 0.71, 0.21,  
295 and 0.60, respectively.”  
296  
297 Answer: [Incorporated in the revised manuscript.](#)  
298  
299 Comment: 42  
300  
301 Page 34232: “Figure 1. b to e represent the seasonal variations of wind direction, wind speed,  
302 relative humidity, and air temperature.”, please keep the consistencies with the context (Page  
303 34208, line 11; lines 18-19). And please add the different symbols of monthly mean variations of  
304 prevailing meteorology from Fig. 1b to 1e.

Answer: Figure 1 is updated as referee suggested.

Comment: 43

The following related citations are recommended to be quoted in the manuscript: [1] Huang, J.\*, W. Zhang, J. Zuo, J. Bi, J. Shi, X. Wang, Z. Chang, Z. Huang, S. Yang, B. Zhang, G. Wang, G. Feng, J. Yuan, L. Zhang, H. Zuo, S. Wang, C. Fu and J. Chou, 2008: An overview of the Semi-Arid Climate and Environment Research Observatory over the Loess Plateau, *Advances in Atmospheric Sciences*, 25(6), 1-16. [2] Wang, G., J. Huang\*, W. Guo, J. Zuo, J. Wang, J. Bi, Z. Huang, and J. Shi, 2010: Observation analysis of land-atmosphere interactions over the Loess Plateau of northwest China, *J. Geophys. Res.*, 115, D00K17, doi:10.1029/2009JD013372. [3] Xie J., J. Huang\*, G. Wang, K. Higuchi, J. Bi, Y. Sun, H. Yu, and T. Wang, 2010: The effects of clouds and aerosols on net ecosystem CO<sub>2</sub> exchange over semi-arid Loess Plateau of Northwest China, *Atmos. Chem. Phys.*, 10, 8205-8218.

Answer: We thank the reviewer for several helpful suggestions and we implemented as suggested.

[1] Huang, J.\*, W. Zhang, J. Zuo, J. Bi, J. Shi, X. Wang, Z. Chang, Z. Huang, S. Yang, B. Zhang, G. Wang, G. Feng, J. Yuan, L. Zhang, H. Zuo, S. Wang, C. Fu and J. Chou, 2008: An overview of the Semi-Arid Climate and Environment Research Observatory over the Loess Plateau, *Advances in Atmospheric Sciences*, 25(6), 1-16.

[2] Wang, G., J. Huang\*, W. Guo, J. Zuo, J. Wang, J. Bi, Z. Huang, and J. Shi, 2010: Observation analysis of land-atmosphere interactions over the Loess Plateau of northwest China, *J. Geophys. Res.*, 115, D00K17, doi:10.1029/2009JD013372.

[3] Xie J., J. Huang\*, G. Wang, K. Higuchi, J. Bi, Y. Sun, H. Yu, and T. Wang, 2010: The effects of clouds and aerosols on net ecosystem CO<sub>2</sub> exchange over semi-arid Loess Plateau of Northwest China, *Atmos. Chem. Phys.*, 10, 8205-8218.



**Influence of Meteorology and interrelationship with greenhouse gases (CO<sub>2</sub> and CH<sub>4</sub>) at a sub-urban site of India**

Sreenivas. G, Mahesh. P\*, Subin Jose, Kanchana A. L., Rao P.V.N, Dadhwal. V.K

Atmospheric and Climate Sciences Group (ACSG),

Earth and Climate Science Area (ECSA),

National Remote Sensing Center (NRSC),

Indian Space Research Organization (ISRO),

Hyderabad, India-500037

\*Corresponding author: Mahesh P

Mail-Id:mahi952@gmail.com

## Abstract

Atmospheric greenhouse gases (GHGs), such as carbon dioxide (CO<sub>2</sub>) and methane (CH<sub>4</sub>), are important climate forcing agents due to their significant impacts on the climate system. The present study brings out first continuous measurements of atmospheric GHGs using high precision Los Gatos Research's greenhouse gas analyser (LGR-GGA) over Shadnagar, a suburban site of Central India during the period 2014. The annual mean of CO<sub>2</sub> and CH<sub>4</sub> over the study region are found to be 394±2.92 ppm and 1.92±0.07 ppm (mean (μ) ± 1std (σ)) respectively. CO<sub>2</sub> and CH<sub>4</sub> showed a significant seasonal variation during the study period with maximum (minimum) CO<sub>2</sub> observed during Pre-monsoon (Monsoon), while CH<sub>4</sub> recorded maximum during post-monsoon and minimum in monsoon. Irrespective of the seasons, consistent diurnal variations of a consistent diurnal mixing ratio of these gases are observed, with high (low) during night (afternoon) hours throughout the study period. Influences of prevailing meteorology (air temperature, wind speed, wind direction and relative humidity) on GHGs have also been investigated. CO<sub>2</sub> and CH<sub>4</sub> showed a strong positive correlation during winter, pre-monsoon, monsoon and post-monsoon with correlation coefficients (Rs) equal to 0.80, 0.80, 0.61 and 0.72 respectively, indicating common anthropogenic source for these gases. It implies the seasonal variations in source-sink mechanisms of CO<sub>2</sub> and CH<sub>4</sub>. Analysis of this study reveals the major sources for CO<sub>2</sub> are soil respiration and anthropogenic emissions while vegetation act as a main sink. Whereas the major source and sink for CH<sub>4</sub> are vegetation and presence of hydroxyl (OH) radicals.

Keywords: Carbon dioxide, Methane, OH radical.

Formatted: Subscript

Formatted: Subscript

## 1. Introduction

The Intergovernmental Panel on Climate Change (IPCC, 2013) reported that humankind is causing global warming through the emission of greenhouse gases (GHGs), particularly carbon dioxide (CO<sub>2</sub>) and methane (CH<sub>4</sub>). CO<sub>2</sub> and CH<sub>4</sub> concentrations have increased by 40% and 150 % respectively since pre-industrial times, mainly from fossil fuel emissions and secondarily from net land use change emissions (IPCC, 2013; Huang et al., 2015). CO<sub>2</sub> measurements at MaunaLoa, Hawaii (Monastersky, 2013) have exceeded the 400 ppm mark several times in May 2013. CH<sub>4</sub> is also receiving increasing attention due to high uncertainty in its sources and sinks (Keppler et al., 2006; Miller et al., 2007; Frankenberg et al., 2008). Stefanie Kirschke et al., (2013) reported that in India, agriculture and waste constitutes the single largest regional source of CH<sub>4</sub>. Although many sources and sinks have been identified for CH<sub>4</sub>, their relative contribution to atmospheric CH<sub>4</sub> is still uncertain (A. Garg et al., 2001; StefanieKirschke et al., 2013). In India, electric power generation ~~that~~ contributes to half of India's total CO<sub>2</sub> equivalent emissions (A. Garg et al., 2001).

Arid and semi-arid areas comprise about 30% of the Earth's land surface. Climate change and climate variability will likely have a significant impact on these regions (Huang et al., 2008; Huang et al., 2015). The variability of environmental factors may result in significant effects on regional climate and global climate (Wang et al., 2010), especially the radiative forcing: via the biogeochemical pathways affecting the terrestrial carbon cycle. Global climate change has serious impact on humans and ecosystems. Due to this, many factors have been identified that may reflect or cause variations in environmental change (Pielke et al., 2002). Out of these, the Normalized Difference Vegetation Index (NDVI) has become one of the most widely used indices to represent the biosphere influence on global change (Liu et al., 2011). ~~The planetary boundary layer (PBL) is the part of the atmosphere closest to the Earth's surface where turbulent processes often dominate the vertical redistribution of sensible heat, moisture, momentum, and aerosols/pollution (AO et al., 2012).~~

Greenhouse and other trace gases have great importance in atmospheric chemistry and for radiation budget of the atmosphere-biosphere system (Crutzen et al., 1991). Hydroxyl radicals (OH) are very reactive oxidizing agents, which are responsible for the oxidation of almost all gases that are emitted by natural and anthropogenic activities in the atmosphere. Atmospheric CO<sub>2</sub> measurements are very important for understanding the carbon cycle because CO<sub>2</sub> mixing ratios

in the atmosphere are strongly affected by photosynthesis, respiration, oxidation of organic matter, biomass and fossil fuel burning, and air–sea exchange process (Machida et al., 2003).

The present study brings out first continuous measurements of atmospheric GHG<sub>2</sub>s using high precision ~~Los Gatos Research's greenhouse gas analyser (LGR-GGA)~~ over Shadnagar, a suburban site of Central India during the period 2014. In addition to GHG<sub>2</sub>s observations, we have also made use of an automatic weather station (AWS) data along with model/satellite retrieved observation during the study period. Details about study area and data sets are described in the following sections.

## 2. Study Area

Shadnagar is situated in Mahabubnagar district of newly formed Indian state of Telangana. It is a ~~rural~~suburban location situated ~70km away from urban site of Hyderabad (Northern side) with a population of ~0.16 million (Patil et al., 2013). A schematic map of study area is shown in Fig. 1a. Major sources of pollutants over Shadnagar can be from small and medium scale industries, biomass burning and bio-fuel as well as from domestic cooking. In the present study sampling of GHG<sub>2</sub>s and related meteorological parameters are carried out in the premises of National Remote Sensing Center (NRSC), ~~Shadnagar~~, Shadnagar Campus (17°02'N, 78°11'E). Sampling site is near (aerial distance ~ 2.25 km) to National highway 7 (NH7) and a railway track (non-electrified) is in the East (E) direction.

Mean monthly variations of temperature (°C) and relative humidity (RH (%)) observed at Shadnagar during 2014 are shown in Figure 1e and 1d respectively. The Indian Meteorological Department (IMD) defined monsoon as June-July-August-September (JJAS), post-monsoon (October-November-December-OND), winter (January-February-JF) and pre-monsoon (March-April-May-MAM) in India. Temperature over Shadnagar varies from ~20°C to ~29°C. Relative humidity (RH) in Shadnagar reached a maximum of ~82 % in monsoon from a minimum of ~48 % recorded during pre-monsoon. Surface wind speed (Fig. 1c) varies between 1.3 to 1.6 m s<sup>-1</sup> with a maximum observed during monsoon and minimum in pre-monsoon. The air mass advecting (Fig. 1b) towards study site is either easterly or westerly. The easterly wind prevails during winter and gradually shifts to south-westerlies in pre-monsoon, and dominates during monsoon.

## 3. Data set and Methodology

Details about the instrument and data utilized are discussed in this section. The availability and frequency of the observations all data used in present study are tabulated in Table 1.

### 3.1 In-situ observations

#### 3.1.1 Greenhouse Gas Analyser (GGA)

The Los Gatos Research's - Greenhouse Gas Analyser (model: LGR-GGA-24EP) is an advanced instrument capable of simultaneous measurements of CO<sub>2</sub>, CH<sub>4</sub> and H<sub>2</sub>O. This instrument is well known for high precision and accuracy which are crucial towards understanding background concentrations of atmospheric GHGs, with specifications meeting WMO standards of measurement (Berman et al., 2012; Shea et al., 2013; Mahesh et al., 2015). It is based on enhanced Off-Axis Integrated Cavity Output Spectroscopy (OA-ICOS) technology (Paul et al. 2001, Baer et al., 2002), which utilizes true wavelength scanning to record fully resolved absorption line shapes. Considering the rural nature of the site, flow rate is fixed to be 7 liters per minute (lpm). Ambient air entering the GGA is analysed using two near infrared (NIR) distributed feedback tunable diode lasers (TDL), one for a CO<sub>2</sub> absorption line near 1.60  $\mu\text{m}$  ( $\nu_0 = 6250\text{ cm}^{-1}$ ) and the other to probe CH<sub>4</sub> and H<sub>2</sub>O absorption lines near 1.65  $\mu\text{m}$  ( $\nu_0 = 6060.60\text{ cm}^{-1}$ ). The concentration of the gases is determined by the absorption of their respective characteristic absorption lines with a high sampling time of 1sec. A detailed explanation regarding the configuration, working and calibration procedure performed for GGA in NRSC can be found elsewhere in Mahesh et al., (2015). In the present study we used GGA retrieved CO<sub>2</sub> and CH<sub>4</sub> data. High resolution data sets are diurnally averaged and is used in further analysis. Due to failure of internal central processing unit (CPU) of the analyzer, data are not recorded from pre-monsoon month of 1<sup>st</sup> May to a few days in 18<sup>th</sup> June during the study period.

#### 3.1.2 O<sub>3</sub> and NO<sub>x</sub> analyzer

Surface concentrations of O<sub>3</sub> and NO<sub>x</sub> have been measured continuously using on-line analyzers (Model No.s: 49i and 42i for O<sub>3</sub> and NO<sub>x</sub> respectively), procured from Thermo Scientific, USA since July 2014. The trace gases (O<sub>3</sub> and NO<sub>x</sub>) sampling inlet is installed on the top of a 2 m mast fixed on the roof of an 8 m high building, and ambient air flow is supplied to the instruments. The inlet prevents the ingress of rain water, and is equipped with 0.5  $\mu\text{m}$  filter to prevent accumulation of dust within the instrument. The ozone analyzer is based on Beer-Lambert-

Formatted: Superscript

Formatted: Superscript

Formatted: Subscript

Formatted: Subscript

Baugher law which relates absorption of light to the concentration of species as its operating principle and has an in-built calibration unit for conducting periodical span and zero checks. The NO<sub>x</sub> analyzer utilizes a molybdenum converter to convert NO<sub>2</sub> into NO and estimates the NO<sub>x</sub> concentration by the intensity of light emitted during the chemiluminescent reaction of NO with O<sub>3</sub> present in the ambient air. The analyzer is integrated with zero and span calibrations which are performed twice monthly.

Simultaneous observations of meteorological parameters are obtained from an automatic weather station (AWS) ~~located in the same campus, installed in NRSC, Shadnagar campus as a part of Calibration and Validation (CAL/VAL) project in March 2012 is equipped with nine sensors to measure fifteen weather parameters. Weather parameters measured are at surface level and height of the AWS mast is ~10 meters. Wind speed and direction measurements are collected at the maximum height (3m) and all others are at 1-1.5m height.~~

Formatted: Line spacing: 1.5 lines

Formatted: Strikethrough

### 3.2 Satellite and Model observations

#### 3.2.1 MODIS

Moderate-resolution Imaging Spectrometer (MODIS) is launched in December 1999 on the polar-orbiting NASA-EOS Terra platform (Salomonson et al. 1989; King et al. 1992). It has 36 spectral channels and acquires data in 3 spatial resolutions of 250 m, 500 m, and 1 km (channels 8–36), covering the visible, near-infrared, shortwave infrared, and thermal-infrared bands. In the present study we used monthly Normalised Difference Vegetation Index (NDVI) data obtained from Terra/MODIS at 5 km spatial resolution. The NDVI value is defined as following ratio of albedos ( $\alpha$ ) at different wavelengths:

$$NDVI = \frac{\alpha_{0.86\mu m} + \alpha_{0.67\mu m}}{\alpha_{0.86\mu m} - \alpha_{0.67\mu m}} \quad (1)$$

NDVI values can range from -1.0 to 1.0 but typical ranges are from 0.1 to 0.7, with higher values associated with greater density and greenness of plant canopies. More details of the processing methods used in generating the data set can be found in James and Kalluri (1994).

#### 3.2.2 COSMIS-RO

COSMIC (Constellation Observation System for Meteorology, Ionosphere and Climate) is a GPS (Global Positioning System) radio occultation (RO) observation system (Wang et al., 2013).

It consists of six identical microsattellites, and was launched successfully on 14 April 2006. GPS radio occultation observation has the advantage of near-global coverage, all-weather capability, high vertical resolution, high accuracy and self-calibration (Yunck et al., 2000). Geophysical parameters ~~(such as, temperature and humidity profiles)~~like temperature and humidity profiles have been simultaneously obtained from refractivity data using one-dimensional variational (1DVAR) analysis. Further COSMIC-RO profiles are used to estimate planetary boundary layer height (BLH). BLH is defined to be the height at which the vertical gradient of the refractivity or water vapor partial pressure is minimum (Ao et al., 2012), explained detail methodology for calculating the BLH from refractivity (N). The planetary boundary layer (PBL) is part of the atmosphere closest to the Earth's surface where turbulent processes often dominate the vertical redistribution of sensible heat, moisture, momentum, and aerosols/pollution (AO et al., 2012).

### 3.2.3 Hysplit model

The general air mass pathway reaching over Shadnagar is analysed using HYSPLIT model (Draxler and Rolph, 2003) [http://www.arl.noaa.gov/ready/hysplit4.html]. We computed 5 day isentropic model backward air mass trajectory for all study days with each trajectory starting at 00:00 UTC and reaching study site, (Shadnagar) at different altitudes (1 km, 2 km, 3 km and 4 km). Even though the trajectory analysis have inherent uncertainties (Stohl, 1998), they are quite useful in determining long range circulation.

## 4. Results and Discussion

### 4.1 Seasonal variations of CO<sub>2</sub> and CH<sub>4</sub>

~~Temporal~~Monthly variations of CO<sub>2</sub> and CH<sub>4</sub> during the study period are shown in Figure. 2a and 2b. The circles indicate the daily mean, while triangular markers represent weekly averages and monthly mean by square markers. Annual mean of CO<sub>2</sub> over study region is found to be  $394 \pm 2.92$  ~~(mean ( $\mu$ )  $\pm$  standard deviation ( $1\sigma$ ))~~( $\mu \pm 1\sigma$ ) ppm with an observed minimum in monsoon and maximum in pre-monsoon. ~~Seasonal mean~~Background (average) values of CO<sub>2</sub> observed during different seasons are  $393 \pm 5.60$ ,  $398 \pm 7.60$ , ~~and~~  $392 \pm 7.0$ , and  $393 \pm 7.0$  ppm ~~in with~~respectively winter, pre-monsoon, monsoon, and post-monsoon respectively. Minimum CO<sub>2</sub> during winter (dry season) ~~can be due to respiratory~~indicates the loss of carbon (Gilmanov et al., 2004; Aurela et al. 2004) as decreased temperature and solar radiation during this period inhibit increases in local CO<sub>2</sub> assimilation (Thum et al., 2009). A steady increase in CO<sub>2</sub> concentration is

observed as season changes from winter to pre-monsoon months. Enhancement in Pre-monsoon is due to higher temperature and solar radiation prevailing during these months which stimulate the assimilation of CO<sub>2</sub> in the daytime and respiration in the night (Fang et al., 2014). The enhanced soil respiration during these months also compliments the increase in CO<sub>2</sub> concentration during this period. In addition to these natural causes, biomass burning over Indian region can also have a significant effect on pre-monsoon CO<sub>2</sub> concentration. More detailed explanation of biomass burning influence on pre-monsoon GHGs concentration is discussed in section 4.6.- Surface CO<sub>2</sub> concentration recorded a minimum during monsoon months can be mainly because of enhanced photosynthesis processes with the availability of greater soil moisture. A decrease in CO<sub>2</sub> concentration is also observed as the monsoon progress. The decreases in temperature (due to cloudy and overcast conditions prevailing during these months) reduce leaf and soil respiration which contributes to the enhancement of carbon uptake (Patil et al., 2013; Jing et al., 2010). Further increase during post-monsoon CO<sub>2</sub> is associated with high ecosystem productivity (Sharma et al., 2014) also an enhancement in soil microbial activity (Stefanie Kirschke et al., 2013).

CH<sub>4</sub> concentration in the troposphere is principally determined by a balance between surface emission and destruction by hydroxyl radicals (OH). The major sources for CH<sub>4</sub> in the Indian region are rice, paddies, wetlands and ruminants (Schneising et al., 2009). Annual CH<sub>4</sub> concentration over study area is observed to be 1.92 ± 0.07 ppm, with a maximum (2.02±0.01 ppm) observed in post-monsoon and minimum (1.85±0.03 ppm) in monsoon. Seasonal mean (average) values of CH<sub>4</sub> observed during different seasons are 1.93±0.05, 1.89±0.05, 1.85±0.03, and 2.02±0.07 ppm with respectively winter, pre-monsoon, monsoon, and post-monsoon. The highest concentration appears during post-monsoon and may be associated with the Kharif season (Goroshiet al., 2011). Seasonal meanBackground (average) values of CH<sub>4</sub> observed during different seasons are 1.93±0.05, 1.89±0.05, and 1.85±0.03, and 2.02±0.07 ppm with respectively winter, pre monsoon, monsoon, and post monsoon. Hayashida et al. (2013) reported that The seasonality of CH<sub>4</sub> concentration over monsoon Asia is characterized by higher values in the wet season and lower values in the dry season; possibly because of the effects of strong emissions from rice paddies and wetlands during the wet season. Low mixing ratios of CH<sub>4</sub> observed during monsoon season were mainly due to the reduction in atmospheric hydrocarbons because of the reduced photochemical reactions and the substantial reduction in solar intensity (Abhishek Gaur et al 2014).The rate of change of CH<sub>4</sub> was found to be high during post-monsoon, and winter. Both



biological and physical processes control the exchange of CH<sub>4</sub> between rice paddy fields and the atmosphere (Nishanth et al., 2014; Goroshiet al., 2011). Due to this, This may be one of the major reasons for the enhanced CH<sub>4</sub> observed during post-monsoon at present study area and winter seasons (Nishanth et al., 2014; Sheshakumar et al., 2011).

#### 4.2 Influence of vegetation on GHGs.

In India cropping season is classified into (i) Kharif and (ii) Rabi based on the onset of monsoon. The Kharif season is from July to October during the south-west (SW) monsoon and Rabi season is from October to March (Koshal Avadhesh, 2013). NDVI being one of the indicators of vegetation change, monthly variations of CO<sub>2</sub> and CH<sub>4</sub> against NDVI is studied to understand the impact of land use land cover on mixing ratios of CO<sub>2</sub> and CH<sub>4</sub>. Monthly mean changes in NDVI, CO<sub>2</sub> and CH<sub>4</sub> are shown in Figure 2c and 2d. Monthly mean of GHGs represented in this analysis is calculated from daily mean in day time (10-16 LT). Analysis of the figure reveals that an inverse relationship exists between NDVI and CO<sub>2</sub>; while a positive relation is observed w.r.t CH<sub>4</sub>. Generally over this part of the country vegetation starts during the month of June with the onset of SW monsoon and as vegetation increases a decrease in CO<sub>2</sub> concentration is observed, due to enhancement in photosynthesis. Further a decline in NDVI is observed as the season advances from post monsoon to winter and then to pre-monsoon, and it is associated with an increase in CO<sub>2</sub> concentration. Similarly, the main source for CH<sub>4</sub> emissions are soil microbial (Stefanie Kirschke et al., 2013) activity which are more active during monsoon and post monsoon seasons. High (low) soil moisture and NDVI is observed in monsoon (pre monsoon) seasons (Figure 8a and 8b). The predominating factors which controls the soil emissions of CO<sub>2</sub>, CH<sub>4</sub> are moisture content, soil temperature, vegetation and soil respiration (Smith et al., 2003; Jones et al., 2005; Chen et al., 2010) respectively.

Biomass burning (forest fire and crop residue burning) is one of the major sources of gaseous pollutants such as carbon monoxide (CO), methane (CH<sub>4</sub>), nitrous oxides (NO<sub>x</sub>) and hydrocarbons in the troposphere (Crutzen et al., 1990, 1985; Sharma et al., 2010). In order to study the role of biomass burning on GHGs a case study is discussed. Figure 43c shows the spatial distribution of MODIS derived fire counts over Indian region during 14-21 April 2014 with air mass trajectories ending over study area over layed on it at different altitudes viz. 1000 m, 2000 m and 4000 m respectively. Analysis of the figure shows a number of potential fire

Formatted: Subscript

Formatted: Subscript

locations on the north-western and south-eastern side of study location and trajectories indicate its possible transport to study area. Daily mean variation of GHGs during the month of April 2014 (Figure 43b) indicates an enhancement in GHGs during the same period (14-21 April 2014). Analysis reveals that CO<sub>2</sub> and CH<sub>4</sub> have increased by ~2% and ~0.06% respectively during event days with respect to monthly mean. This analysis reveals that long range / regional transported biomass burning have a role in enhancement of GHGs over study site. Further to understand the seasonal variation of biomass burning contribution to GHGs we analysed long term (2003-2013) Fire Energetics and Emissions Research version 1.0 (FEER v1) data over study area. Emission coefficient (C<sub>e</sub>) products during biomass burning is developed from coincident measurements of fire radiative power (FRP) and AOD from MODIS Aqua and Terra satellites (Ichoku and Ellison, 2014). Figure 43a shows seasonal variation of CO<sub>2</sub> emission due to biomass burning over the study site. Enhancement in CO<sub>2</sub> emission is seen during pre-monsoon months; which also supports earlier observation (Figure 2a). This analysis reveals that biomass burning has a role in pre-monsoon enhancement of CO<sub>2</sub> over study site. For a qualitative analysis of this long range transport, we have analysed air mass trajectories ending over study site during different seasons.

#### **4.3 Correlation between CO<sub>2</sub> and CH<sub>4</sub>**

A correlation study is carried out between hourly averaged CO<sub>2</sub> and CH<sub>4</sub> during all season for the entire study period. The statistical analysis for different seasons is shown in Table 32. Fang et al., (2015) suggest the correlation coefficients (Rs) value higher than 0.50 indicates a similar source mechanism of CO<sub>2</sub> and CH<sub>4</sub>. Also a positive correlation dominance of anthropogenic emission on carbon cycle. Our study also reveals a strong positive correlation observed between CO<sub>2</sub> and CH<sub>4</sub> during winter, pre-monsoon, monsoon, and post-monsoon with R equal to 0.80, 0.80, 0.61, and 0.72 respectively. Seasonal regression coefficients (slope) and their uncertainties ( $\Psi_{\text{slope}}$ ,  $\Psi_{\text{y-int}}$ ) are computed using Taylor (1997) which showed maximum during winter, pre-monsoon, and minimum in a monsoon that figure out the hourly stability of the mixing ratios between CO<sub>2</sub> and CH<sub>4</sub>. This can be due to relatively simple source/sink process of CO<sub>2</sub> in comparison with CH<sub>4</sub>. Figure 54 shows the seasonal variation of  $\Delta\text{CH}_4/\Delta\text{CO}_2$ . Dilution effects during transport of CH<sub>4</sub> and CO<sub>2</sub> can be minimized to some extent by dividing the increase of CH<sub>4</sub> over time by the respective increase in CO<sub>2</sub> (Worthy et al., 2009). In this study, background concentrations of

respective GHGs are determined as mean values of the 1.25 percentile of data for monsoon, post-monsoon, pre-monsoon and winter (Pan et al., 2011; Worthy et al., 2009). Annual  $\Delta\text{CH}_4/\Delta\text{CO}_2$  over the study region during the study period is found to be 7.1 (ppb/ppm). This low value clearly indicates the dominance of  $\text{CO}_2$  over the study region. The reported  $\Delta\text{CH}_4/\Delta\text{CO}_2$  values from some of the rural sites viz Canadian Arctic and Hateruma Island (China) are of the order 12.2 and ~10 ppb/ppm respectively (Worthy et al., 2009; Tohjima et al., 2014). Average  $\Delta\text{CH}_4/\Delta\text{CO}_2$  ratio during winter, pre-monsoon, monsoon and post-monsoon are 9.40, 6.40, 4.40, and 8.20 ppb respectively. Monthly average, of  $\Delta\text{CH}_4/\Delta\text{CO}_2$ , is relatively high from late post-monsoon to winter, when the biotic activity is relatively dormant (Tohjima et al., 2014). During pre-monsoon decrease in  $\Delta\text{CH}_4/\Delta\text{CO}_2$  ratio indicates the enhancement of  $\text{CO}_2$  relative to that of  $\text{CH}_4$ .

#### 4.2.4.4 Diurnal variations of $\text{CO}_2$ and $\text{CH}_4$

Figure 25ea to 5d and 2d shows the seasonally averaged diurnal cycle of  $\text{CO}_2$  and  $\text{CH}_4$  over Shadnagar during study period. The vertically bar represents the standard deviation from respective mean. Irrespective of seasonal variation GHGs showed a similar diurnal variation, with maximum mixing ratios observed during early morning (06:00 hrs) as well as early night hours (20:00 hrs) and minimum during afternoon hours. Figure 2e and 2d depicts seasonal diurnal variations of  $\text{CO}_2$  and  $\text{CH}_4$  over Shadnagar during study period. The amplitudes diurnal changes during seasonal variation mainly depend on biosphere sources and sinks such as land use and land cover change (Fearnside 2000, IPCC, and AR5). Maximum mixing ratios of  $\text{CO}_2$  and  $\text{CH}_4$  are observed during early morning and late night hours. Peak surface concentrations of  $\text{CO}_2$  and  $\text{CH}_4$  increase at night and remain high until sunrise (22:00hrs to 06:00hrs). However the difference observed in the maximum diurnal amplitudes can be attributed to seasonal changes. The observed diurnal cycle of GHGs is closely associated with diurnal variation of planetary boundary layer height (PBLH). For better understanding of the diurnal behavior of  $\text{CO}_2/\text{CH}_4$ , we used European Centre for Medium-range Weather Forecasting (ECMWF) Interim Reanalysis (ERA) PBL data set which gives the data for every three hours viz. 00:00, 03:00, 06:00, 09:00, 12:00, 15:00, 18:00, and 21:00 UTC with a resolution of  $0.25^\circ \times 0.25^\circ$  (<http://data-portal.ecmwf.int>). Figure 5a to 5d portrays the diurnal evolution of  $\text{CO}_2/\text{CH}_4$  during different season along with the evolution of Boundary Layer Height (m) on secondary y axis. The morning peak arises due to combined

Formatted: Subscript

Formatted: Subscript

Formatted: Subscript

Formatted: Subscript

influence of fumigation effect, (Stull 1988) and morning build-up of local anthropogenic activities (household and vehicular transport). Low value of GHGs as the day progress can be attributed to increased photosynthetic activity during day time and destruction of stable boundary layer and residual layer due convective activity. In the evening hours, surface inversion begins and form a shallow stable boundary layer (Nair et al., 2007) causing the enhancement in GHGs concentration near the surface. Figure 2e shows mixing ratios of CO<sub>2</sub> are gradually decreasing after sun rise and reaching peak minimum in the afternoon because of the net ecosystem uptake of the biosphere and boundary layer dynamics. During night time, mixing ratios increase due to formation of stable atmospheric boundary layer, soil respiration of the biosphere and absence of photosynthetic activity. Similar trend in diurnal variation of GHG's is reported from other parts of the country (Patil et al., 2013; Mahesh et al., 2014; Sharma et al., 2014; Nishanth et al., 2014). Although diurnal variations of CH<sub>4</sub> showed similar trend as of CO<sub>2</sub>, but are caused due to different factors. Lower troposphere acts as main sink for CH<sub>4</sub> with the formation of O<sub>3</sub> through oxidation of CH<sub>4</sub> and other trace species in the presence of NO<sub>x</sub> and hydroxyl radicals (OH) (Eisele et al., 1997, IPCC, AR5).

#### 4.3.4.5 Influence of prevailing meteorology

Redistribution (both horizontal and vertical) of GHG's also plays a role in their seasonal variation, as it controls transport and diffusion of pollutants from one place to another (Hassan 2015). A good inverse correlation between wind speed and GHG's suggest the proximity of sources near measurement site, while a not so significant correlation suggests the influence of regional transport (Ramachandran and Rajesh, 2007). Figure 3a and 3b shows scatter plot between GHG's and wind speed during different seasons. Analysis of Figure 3 shows that there exists an inverse correlation between daily mean wind speed and GHG's. Correlation coefficients (R<sub>s</sub>) between wind speed and CO<sub>2</sub> during pre-monsoon, monsoon, post-monsoon, and winter is 0.56, 0.32, 0.06, and 0.67 respectively. While for CH<sub>4</sub> it is found be 0.28, 0.71, 0.21, and 0.60 respectively. Negative correlation indicates that the influence of local sources on GHG's, however, poor correlation coefficients during different seasons suggest the role of regional/local transport (Mahesh et al 2014). Also an understanding of prevailing wind direction and its relationship with GHG's helps in determining their probable source regions. Table 23 shows the monthly mean variation of CO<sub>2</sub> and CH<sub>4</sub> with respect to different wind direction. Enhancement in CO<sub>2</sub> and CH<sub>4</sub> level over Shadnagar are observed to mainly come from NW and NE while the

lowest is from the S and SW. This can be associated to some extent with industrial emissions located in western side of sampling site, and the influence of emission and transport from nearby urban center on the NW side of the study site.

The influence of meteorological parameters (temperature and relative humidity) influence on trace gases is also examined. Figure 47a and 7b (top panel corresponds to CO<sub>2</sub> and bottom panel represents CH<sub>4</sub>) shows the scatter plot of temperature ~~versus~~ relative humidity as a function of GHGs during different seasons. ~~Here, d~~ Daily mean data is used instead of hourly mean data, to avoid the influence of the diurnal variations on correlations. CO<sub>2</sub> showed a positive correlation with temperature during all season except during winter. This negative correlation can be attributed to different response of photosynthesis rate to different air temperature decrease in rate of photosynthesis. IPCC (1990) reports that many mid-latitude plants shows an optimum gross photosynthesis rate when temperature varied from of 20 to 35 °C. The rate of plant respiration tends to be slow below 20°C. However, at higher temperatures, the respiration rate accelerates rapidly up to a temperature at which, it equals the rate of gross photosynthesis and there can be no net assimilation of carbon. While CH<sub>4</sub> showed a weak positive correlation with temperature during pre-monsoon and post-monsoon, while a weak negative correlation is observed during monsoon and winter. This could be due to the rate of chemical loss reaction with OH is faster in summer and minimum in other seasons. A case study on CH<sub>4</sub> sink mechanism has discussed in section 4.6. ~~This indicates that regional air temperature doesn't significantly influence seasonal variation of CH<sub>4</sub> (Chen et al., 2015).~~ Seasonal variation of GHG<sup>2</sup>s also showed an insignificantly negative correlation with relative humidity. ~~A similar observation is also reported by Abhishek et al., (2014).~~ One of the supporting argument can be in humid conditions, these stoma can fully open to increase the uptake of CO<sub>2</sub> without a net water loss. Also, wetter soils can promote decomposition of dead plant materials, releasing natural fertilizers that help plants grow (Abhishek et al., 2014).

Figure 8a and 8b illustrates the daily mean variation of GHGs with respect to soil moisture and soil temperature (Top panel represent the seasonal variation of CO<sub>2</sub> w.r.t soil moisture and soil temperature, while bottom panel represent the seasonal variation of CH<sub>4</sub> against the same parameters with the same). It's quite interesting to observe that GHGs behave differently w.r.t soil moisture during different seasons. CH<sub>4</sub> shows a positive relationship during monsoon and post-monsoon and an inverse relationship exist during pre-monsoon and winter; while a reverse

Formatted: Subscript

relationship exist for CO<sub>2</sub>. During wet season aeration is restricted (Smith et al. 2003) hence soil respiration is limited, which decrease CO<sub>2</sub> flux. This can be one of the factors for low values of CO<sub>2</sub> during monsoon months, during dry months soil may act as sink of CH<sub>4</sub>.

#### **4.3.14.5.1 Influence of boundary layer height on GHGs mixing ratios**

The planetary boundary layer is the lowest layer of the troposphere where wind speed as a function of temperature plays major role in its thickness variation. It is an important parameter for controlling the observed diurnal variations and potentially masking the emissions signal (Newman et al., 2013). Since complete set of COSMIC RO data is not available during the study period, in this analysis we have analysed RO data from July 2013 to June 2014, along with simultaneous observations of GHG's. Monthly variations (Figure not show) of BLH computed from high vertical resolution of COSMIC-RO data against CO<sub>2</sub> and CH<sub>4</sub> concentrations. Monthly BLH is observed to be minimum (maximum) during winter and monsoon (pre monsoon) seasons and it closely resembles with the air temperature pattern. The highest (lowest) BLH over study region was identified 3.20 km (1.50 km). A monthly average monthly air temperature is maximum (minimum) of 29°C (20°C) during the summer (winter) months.

Seasonal BLH during winter, pre-monsoon, monsoon and post monsoon are 2.10 km, 3.15 km, 1.74 km and 2.30 km respectively. change in BLH thickness over study region was observed to be as Monsoon (M, 1.74 km) < winter (W, 2.10 km) < Post Monsoon (PM, 2.30 km) < Pre-monsoon (Pre-M, 3.15 km); its influence on CO<sub>2</sub> and CH<sub>4</sub> mixing ratios are shown in Figure 59a and 59b. X axis represents the seasonal transition i.e. monsoon to post monsoon (M-PM) etc and y axis indicates seasonal difference of BLH and GHGs concentration respectively. As seasonal BLH thickness increase, mixing ratios of CO<sub>2</sub> (CH<sub>4</sub>) decreased from 8.68 ppm to 5.86 ppm (110 ppb to 40 ppb). This effect clearly captured by seasonal diurnal averaged BLH data sets used from ECMWF-ERA. The amount of biosphere emissions influence on CO<sub>2</sub> and CH<sub>4</sub> can be estimated through atmospheric boundary layer processes. Since the study region being a flat terrain, variations in CO<sub>2</sub> and CH<sub>4</sub> were mostly influenced by boundary layer BLH thickness through convection and biosphere activities.

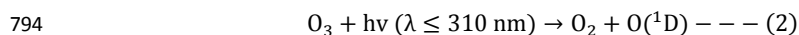
#### **4.4 Correlation between CO<sub>2</sub> and CH<sub>4</sub>**

A correlation study is carried out between hourly averaged  $\text{CO}_2$  and  $\text{CH}_4$  during all season for the entire study period. The statistical analysis for different seasons is shown in Table 3. Fang et al., (2015) suggest the correlation coefficient (R) value higher than 0.50 indicates a similar source mechanism of  $\text{CO}_2$  and  $\text{CH}_4$ . Also a positive correlation dominance of anthropogenic emission on carbon cycle. Our study also reveals a strong positive correlation observed between  $\text{CO}_2$  and  $\text{CH}_4$  during winter, pre-monsoon, monsoon and post-monsoon with R equal to 0.80, 0.80, 0.61 and 0.72 respectively. Seasonal regression coefficients (slope) and their uncertainties ( $\psi_{\text{slope}}$ ,  $\psi_{y\text{-int}}$ ) are computed using Taylor (1997) which showed maximum during winter, pre-monsoon and minimum in a monsoon that figure out the hourly stability of the mixing ratios between  $\text{CO}_2$  and  $\text{CH}_4$ . This can be due to relatively simple source/sink process of  $\text{CO}_2$  in comparison with  $\text{CH}_4$ . Dilution effects during transport of  $\text{CH}_4$  and  $\text{CO}_2$  can be minimized to some extent by dividing the increase of  $\text{CH}_4$  over time by the respective increase in  $\text{CO}_2$  (Worthy et al., 2009). Figure 6 shows the seasonal variation of  $\Delta\text{CH}_4/\Delta\text{CO}_2$ . In this study, background concentrations of respective GHG's are determined as mean values of the 1.25 percentile of data for monsoon, post-monsoon, pre-monsoon and winter (Pan et al., 2011; Worthy et al., 2009). Annual  $\Delta\text{CH}_4/\Delta\text{CO}_2$  over the study region during the study period is found to be 7.1 (ppb/ppm). This low value clearly indicates the dominance of  $\text{CO}_2$  over the study region. The reported  $\Delta\text{CH}_4/\Delta\text{CO}_2$  values from some of the rural sites viz Canadian Arctic and Hateruma Island (China) is of the order 12.2 and 10 ppb/ppm respectively (Worthy et al., 2009; Tohjima et al., 2014). Average  $\Delta\text{CH}_4/\Delta\text{CO}_2$  ratio during winter, pre-monsoon, monsoon and post-monsoon are 9.40, 6.40, 4.40, and 8.20 ppb respectively. Monthly average, of  $\Delta\text{CH}_4/\Delta\text{CO}_2$ , is relatively high from late post-monsoon to winter, when the biotic activity is relatively dormant (Tohjima et al., 2014). During pre-monsoon decrease in  $\Delta\text{CH}_4/\Delta\text{CO}_2$  ratio indicates the enhancement of  $\text{CO}_2$  relative to that of  $\text{CH}_4$ .

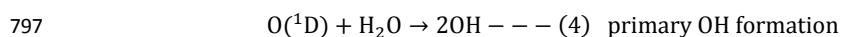
#### 4.5.4.6 Methane ( $\text{CH}_4$ ) sink mechanism

Methane ( $\text{CH}_4$ ) is the most powerful greenhouse gas after  $\text{CO}_2$  in the atmosphere due to its strong positive radiative forcing (IPCC, AR5). Atmospheric  $\text{CH}_4$  is mainly (70-80%) from biological origin produced in anoxic environments, by anaerobic digestion of organic matter (Crutzen and Zimmermann, 1991). The major  $\text{CH}_4$  sink is oxidation by hydroxyl radicals (OH), which accounts for 90 % of  $\text{CH}_4$  sink (Vaghjani and Ravishankara, 1991; Kim et al., 2015). OH radicals are very reactive and are responsible for the oxidation of almost all gases in the

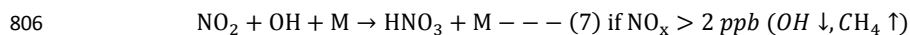
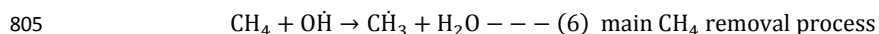
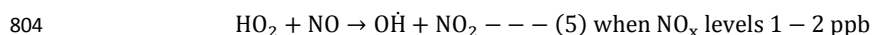
791 atmosphere. Primary source for OH radical formation in the atmosphere is photolysis of ozone  
 792 (O<sub>3</sub>) and water vapor (H<sub>2</sub>O). Eisele et al., (1997) defined primary and secondary source of OH  
 793 radicals in the atmosphere. Primary source of OH radical is as follows;



795 where O(^1D) is electronically excited atom



798 Removal of CH<sub>4</sub> is constrained by the presence of OH radicals in the atmosphere. A 1 min time  
 799 series analysis of CH<sub>4</sub>, NO<sub>x</sub>, O<sub>3</sub> and H<sub>2</sub>O and associated wind vector for August 2014 to understand  
 800 the CH<sub>4</sub> chemistry is shown in Figure 710a and Figure 710b. Low NO<sub>x</sub> (1-2 ppb) values are shown  
 801 in horizontal elliptical region of Figure 710a and observed corresponding low CH<sub>4</sub> (1.80 ppm)  
 802 concentrations. The low NO<sub>x</sub> in turn produces high OH radicals in the atmosphere due to  
 803 conversion of HO<sub>2</sub> radical by NO, which removes CH<sub>4</sub> through oxidation process as shown below.



807 Crutzen and Zimmermann, (1991) and Eisele et al., (1997) observed that at low NO<sub>x</sub> (0.5-2.0 ppb)  
 808 levels most HO<sub>x</sub> family radicals such as HO<sub>2</sub> and peroxy radicals (RO<sub>2</sub>) react with NO to form OH  
 809 radicals. Therefore OH radicals are much higher in the case of low NO<sub>x</sub>. When NO<sub>x</sub> levels increase  
 810 more than 2 ppb, most of the OH radicals react with NO<sub>2</sub> to form nitric acid (HNO<sub>3</sub>). In first order,  
 811 the levels of CH<sub>4</sub> in the atmosphere depend on the levels of NO<sub>x</sub> though the production of OH  
 812 radicals in the atmosphere is still uncertain. Figure 710a and 710b showed high CH<sub>4</sub>, H<sub>2</sub>O, O<sub>3</sub> and  
 813 NO<sub>x</sub> during a few days in August 2014. High concentrations of CH<sub>4</sub>, NO<sub>x</sub> and other gases are  
 814 observed in the eastern direction of study site. Very high NO<sub>x</sub> levels above 10 ppb are observed  
 815 and subsequently CH<sub>4</sub> concentrations also increased to 2.40 ppm from 1.80 ppm. In the eastern



direction of study site a national highway and single line broad gauge railway network are present which act as possible sources of NO<sub>x</sub>, CH<sub>4</sub> and CO<sub>2</sub>. Increase in emissions of NO<sub>x</sub> causes decline in the levels of OH radicals and subsequently observed high CH<sub>4</sub> over the study region.

#### ~~4.6 Influence of vegetation on GHG's.~~

~~In India cropping season is classified into (i) Kharif and (ii) Rabi based on the onset of monsoon. The kharif Kharif season is from July to October during the south west monsoon and Rabi season is from October to March (Avadhesh Koshal, 2013). NDVI being one of the indicators of vegetation change, monthly variations of CO<sub>2</sub> and CH<sub>4</sub> against NDVI is studied to understand the impact of land use land cover on mixing ratios of CO<sub>2</sub> and CH<sub>4</sub>. Monthly changes in NDVI, CO<sub>2</sub> and CH<sub>4</sub> are shown in Figure 8. Monthly mean of GHG's represented in this analysis is calculated from daily day time (10-16 LT) mean. Maximum NDVI of 0.60 corresponding to the minimum CO<sub>2</sub> concentration (about 382 ppm) is observed in September. NDVI showed inverse relationship with CO<sub>2</sub>, mainly due to change in vegetation which affects the CO<sub>2</sub> concentrations. Initially during the month of June vegetation start increasing with availability of water and as vegetation increases, concentration. Similarly, The main source for CH<sub>4</sub> emissions are soil microbial (Stefanie Kirschke et al., 2013) activity which are more active during monsoon and post monsoon seasons. High (low) soil moisture and NDVI is observed in monsoon (pre monsoon) seasons (Figure 9a and b). The predominating factors which controls the soil emissions of CO<sub>2</sub>, CH<sub>4</sub> are moisture content, soil temperature, vegetation and soil respiration (Smith et al., 2003; Jones et al., 2005; Chen et al., 2010) respectively.~~

~~Biomass burning (forest fire and crop residue burning) is one of the major sources of gaseous pollutants such as carbon monoxide (CO), methane (CH<sub>4</sub>), nitrous oxides (NO<sub>x</sub>) and hydrocarbons in the troposphere (Crutzen et al., 1990, 1985; Sharma et al., 2010). In order to study the role of biomass burning on GHG's a case study is discussed. Figure 10a shows the spatial distribution of MODIS derived fire counts over Indian region during 14-21 April 2014 with air mass trajectories ending over study area over layed on it at different altitudes viz. 1000m, 2000m and 4000m respectively. Analysis of the figure shows a number of potential fire locations on the north western and south eastern side of study location and trajectories indicates its possible transport to study area. Daily mean variation of GHGs during the month of April 2014 (Figure~~

Formatted: Strikethrough

10b) indicates an enhancement in GHGs during the same period (14–21 April 2014). Analysis reveals that CO<sub>2</sub> and CH<sub>4</sub> has increased by ~2% and ~0.06% respectively during event days with respect to monthly mean. This analysis reveals that long range / regional transported biomass burning have a role in enhancement of GHGs over study site. Further to understand the seasonal variation of biomass burning contribution to GHGs we analysed over study site we have analysed GHG's emissions from biomass burning using long term (2003–2013) Fire Energetics and Emissions Research version 1.0 (FEER-v1) data over study area. Emission coefficient (C<sub>e</sub>) products during biomass burning is developed from coincident measurements of fire radiative power (FRP) and AOD from MODIS Aqua and Terra satellites (Ichoku and Ellison, 2014). Figure 10c shows seasonal variation of CO<sub>2</sub> emission due to biomass burning over the study site. Enhancement in CO<sub>2</sub> emission is seen during pre-monsoon months; which also supports earlier observation (Figure 2a). This analysis reveals that biomass burning has a role in pre-monsoon enhancement of CO<sub>2</sub> over study site. For a qualitative analysis of this long-range transport, we have analysed air mass trajectories ending over study site during different seasons.

Formatted: Subscript

#### 4.7 Long range circulations

To understand the role of long range circulation, we separated the trajectory into 4 clusters based on their pathway, namely North-East (N-E), North-West (N-W), South-East (S-E), South-West (S-W). The main criterion of trajectory clustering is to minimize the variability among trajectories and maximize variability among clusters. Cluster mean trajectories of air mass and their percentage contribution to the total calculated for each season over the study period at 3 Km altitude are depicted in Figure 911. Majority of air mass trajectories during winter (~44%), pre-monsoon (~64%), monsoon (~80%) and post-monsoon (~41%) are originating from NW parts of the study site. For a comprehensive analysis, percentage occurrences of cluster mean trajectories of air mass over study area during different season at different altitudes are also tabulated in Table 4. During post-monsoon to early pre-monsoon periods which are generally the post-harvest period for some of the crops agriculture residue burning which are quite common in the NW and NE regions part of India (Sharma et al, 2010). Our analysis reveals that during this period majority of air mass reaching the study site at different altitudes come from this part of the country.

## 5. Conclusions

The present study analysed the seasonal variations of atmospheric GHG<sup>2</sup>s (CO<sub>2</sub> and CH<sub>4</sub>) and associated prevailing meteorology over Shadnagar, a suburban site of Central India during the period 2014. The salient findings of the study are the following:

- Irrespective of seasons, major sources for CO<sub>2</sub> are soil respiration and anthropogenic emissions while vegetation acts as a main sink. Whereas the major source and sink for CH<sub>4</sub> are vegetation and presence of hydroxyl (OH) radicals. In addition, boundary layer dynamics and long range transport also plays a vital role on GHGs mixing ratios.
- The annual mean of CO<sub>2</sub> and CH<sub>4</sub> over the study region ~~are~~<sup>is</sup> found to be 394±2.92 ppm and 1.92±0.07 ppm ( $\mu\pm 1\sigma$ ) respectively. CO<sub>2</sub> and CH<sub>4</sub> showed a significant seasonal variation during the study period. Maximum (Minimum) CO<sub>2</sub> is observed during Pre-monsoon (Monsoon), while CH<sub>4</sub> recorded maximum during post-monsoon and minimum in monsoon. Seasonal analysis of FEER data also showed maximum emission of CO<sub>2</sub> due to biomass burning during pre-monsoon months which indicates the influence of biomass burning on local emissions.
- CO<sub>2</sub> and CH<sub>4</sub> showed consistent diurnal behavior in spite of their significant seasonal variations, with an observed morning (06:00 IST) maxima, followed by afternoon minima (14:00 IST) and enhancing in the late evening (~22:00 IST).
- Correlation coefficient ( $R_s$ ) between wind speed and CO<sub>2</sub> during pre-monsoon, monsoon, post-monsoon and winter is 0.56, 0.32, 0.06 and 0.67 respectively. While for CH<sub>4</sub> it is found be 0.28, 0.71, 0.21, and 0.60 respectively. Negative correlation indicates that the influence of local sources on GHG<sup>2</sup>s, however, poor correlation coefficients during different seasons suggest the role of regional/local transport.
- CO<sub>2</sub> showed a positive correlation with temperature during all seasons except during winter. ~~Where as~~<sup>Whereas</sup> CH<sub>4</sub> showed a weak positive correlation with temperature during pre-monsoon and post-monsoon, while showing a weak negative correlation during monsoon and winter.
- CO<sub>2</sub> and CH<sub>4</sub> showed a strong positive correlation during winter, pre-monsoon, monsoon and post-monsoon with  $R_s$  equal to 0.80, 0.80, 0.61 and 0.72 respectively. This clearly

Formatted: Font: (Default) Times New Roman, 12 pt

indicates [common anthropogenic sources for these gases](#),~~the seasonal variations in source-sink mechanisms of CO<sub>2</sub> and CH<sub>4</sub> respectively.~~

- ~~• Presence of OH radicals has been implicitly confirmed as a major sink of CH<sub>4</sub> over the study region.~~

## Acknowledgment

This work was part of the Atmospheric CO<sub>2</sub> Retrieval and Monitoring (ACRM) under National Carbon Project (NCP) of ISRO-GBP. [Authors sincerely acknowledge Mr. Biswadip Gharai, ACSG/ECSA for providing LULC data and to Mr. Mallikarjun, ACSG/ECSA for his support in data collection.](#) We thank D & PQE division of NRSC and Mrs. Sujatha P, ACSG for sharing AWS and boundary layer data. The authors are grateful to the AT-CTM project of ISRO-GBP for providing the O<sub>3</sub> and NO<sub>x</sub> analyzers. We would also like to thank [HYSPLIT](#), [ECMWF-ERA](#), MODIS and COSMIC team for providing scientific data sets used in this study. [We also thankful to anonymous referees and the editor for providing constructive suggestions which certainly improved the quality of manuscript.](#)

## References

Ao, C. O., Waliser, D. E., Chan, S. K., Li, J. L., Tian, B., Xie, F., & Mannucci, A. J. Planetary boundary layer heights from GPS radio occultation refractivity and humidity profiles. *Journal of Geophysical Research: Atmospheres* (1984–2012), 117(D16), (2012).

[Aurela M, Lohila A, Tuovinen JP, Hatakka J, Riutta T, Laurila T \(2009\) Carbon dioxide exchange on a northern boreal fen. \*Boreal Environment Research\* 14\(4\): 699-710](#)

Baer, D. S., Paul, J. B., Gupta, M., & O'Keefe, A. Sensitive absorption measurements in the near-infrared region using off-axis integrated cavity output spectroscopy. In *International Symposium on Optical Science and Technology* (pp. 167-176). International Society for Optics and Photonics, (2002).

Berman, E. S., Fladeland, M., Liem, J., Kolyer, R., & Gupta, M. Greenhouse gas analyzer for measurements of carbon dioxide, methane, and water vapor aboard an unmanned aerial vehicle. *Sensors and Actuators B: Chemical*, 169, 128-135, (2012).

932 Chen, H., Wu, N., Wang, Y., & Peng, C. Methane is an Important Greenhouse Gas. Methane  
 933 Emissions from Unique Wetlands in China: Case Studies, Meta Analyses and Modelling, chapter  
 934 1, (2015).

935 Crutzen, P. J., & Andreae, M. O. Biomass burning in the tropics: Impact on atmospheric chemistry  
 936 and biogeochemical cycles. *Science*, 250(4988), 1669-1678, (1990).

937 Crutzen, P. J., A. C. Delany, J. Greenberg, P. Haagenson, L. Heidt, R. Lueb, W. Pollock, Wartburg  
 938 Seiler, A. Wartburg, and P. Zimmerman. "Tropospheric chemical composition measurements in  
 939 Brazil during the dry season." *Journal of Atmospheric Chemistry* 2, no. 3 (1985): 233-256.  
 940 Draxler RR, Rolph GD. HySPLIT (Hybrid Single Particle Lagrangian Integrated Trajectory)  
 941 Model access via NOAA ARL READY website (<http://www.arl.noaa.gov/ready/hysplit4.html>),  
 942 NOAA Air Resources Laboratory. *Silver Spring, MD*. 2003.

943  
 944 Eisele, F. L., Mount, G. H., Tanner, D., Jefferson, A., Shetter, R., Harder, J. W., & Williams, E. J.  
 945 Understanding the production and interconversion of the hydroxyl radical during the Tropospheric  
 946 OH Photochemistry Experiment. *Journal of Geophysical Research: Atmospheres* (1984–2012),  
 947 102(D5), 6457-6465, (1997).

948 Fang, S. X., L. X. Zhou, P. P. Tans, P. Ciais, M. Steinbacher, L. Xu, and T. Luan. "In situ  
 949 measurement of atmospheric CO<sub>2</sub> at the four WMO/GAW stations in China." *Atmospheric  
 950 Chemistry and Physics* 14, no. 5 (2014): 2541-2554.

951 Fang, S. X., P. P. Tans, M. Steinbacher, L. X. Zhou, and T. Luan. "Study of the regional CO<sub>2</sub> mole  
 952 fractions filtering approach at a WMO/GAW regional station in China." *Atmospheric  
 953 Measurement Techniques Discussions* 8, no. 7 (2015).

954 [Fearnside, Philip M. "Global warming and tropical land use change: greenhouse gas emissions  
 955 from biomass burning, decomposition and soils in forest conversion, shifting cultivation and  
 956 secondary vegetation." \*Climatic change\* 46, no. 1-2 \(2000\): 115-158.](#)

957 Frankenberg, Christian, Peter Bergamaschi, André Butz, Sander Houweling, Jan Fokke Meirink,  
 958 Justus Notholt, Anna Katinka Petersen, Hans Schrijver, Thorsten Warneke, and Ilse Aben.  
 959 "Tropical methane emissions: A revised view from SCIAMACHY onboard ENVISAT."  
 960 *Geophysical Research Letters* 35, no. 15 (2008).

961 Garg, A., Bhattacharya, S., Shukla, P. R., & Dadhwal, V. K. Regional and sectoral assessment of  
 962 greenhouse gas emissions in India. *Atmospheric Environment*, 35(15), 2679-2695, (2001).

963  
 964 Gaur, A., Tripathi, S. N., Kanawade, V. P., Tare, V., & Shukla, S. P. Four-year measurements of  
 965 trace gases (SO<sub>2</sub>, NO<sub>x</sub>, CO, and O<sub>3</sub>) at an urban location, Kanpur, in Northern India. *Journal of  
 966 Atmospheric Chemistry*, 71(4), 283-301, (2014).

967

968 Gilmanov, T. G., Johnson, D. A., Saliendra, N. Z., Akshalov, K., & Wylie, B. K. Gross primary  
 969 productivity of the true steppe in Central Asia in relation to NDVI: scaling up CO<sub>2</sub> fluxes.  
 970 *Environmental Management*, 33(1), S492-S508, (2004).

971 Goroshi, S. K., Singh, R. P., Panigrahy, S., & Parihar, J. S. Analysis of seasonal variability of  
 972 vegetation and methane concentration over India using SPOT-VEGETATION and ENVISAT-  
 973 SCIAMACHY data. *Journal of the Indian Society of Remote Sensing*, 39(3), 315-321, (2011).

974  
 975 Hassan, A. G. A. Diurnal and Monthly Variations in Atmospheric CO<sub>2</sub> Level in Qena, Upper  
 976 Egypt. *Resources and Environment*, 5(2), 59-65, (2015).

977  
 978 [Hayashida, S., Ono, A., Yoshizaki, S., Frankenberg, C., Takeuchi, W., & Yan, X. \(2013\). Methane](#)  
 979 [concentrations over Monsoon Asia as observed by SCIAMACHY: Signals of methane emission](#)  
 980 [from rice cultivation. \*Remote Sensing of Environment\*, 139, 246-256.](#)

981  
 982 [Huang, J.\\*, W. Zhang, J. Zuo, J. Bi, J. Shi, X. Wang, Z. Chang, Z. Huang, S. Yang, B. Zhang, G.](#)  
 983 [Wang, G. Feng, J. Yuan, L. Zhang, H. Zuo, S. Wang, C. Fu and J. Chou, 2008: An overview of](#)  
 984 [the Semi-Arid Climate and Environment Research Observatory over the Loess Plateau. \*Advances\*](#)  
 985 [in Atmospheric Sciences, 25\(6\), 1-16.](#)

986  
 987 [Huang, J., Yu, H., Guan, X., Wang, G., & Guo, R. \(2015\). Accelerated dryland expansion under](#)  
 988 [climate change. \*Nature Climate Change\*. doi:10.1038/nclimate2837.](#)

989  
 990 Ichoku, C., & Ellison, L. Global top-down smoke-aerosol emissions estimation using satellite fire  
 991 radiative power measurements. *Atmospheric Chemistry and Physics*, 14(13), 6643-6667, (2014).

992 Intergovernmental Panel on Climate Change (IPCC). Climate Change: The IPCC Scientific  
 993 Assessment, edited by J. T. Houghton, G. J. Jerkins and J. J. Ephraums. Cambridge University  
 994 Press. New York, (IPCC, 1990).

995 James, M. E., & Kalluri, S. N. The Pathfinder AVHRR land data set: an improved coarse resolution  
 996 data set for terrestrial monitoring. *International Journal of Remote Sensing*, 15(17), 3347-3363,  
 997 (1994).

998 [Jing, X., Huang, J., Wang, G., Higuchi, K., Bi, J., Sun, Y., ... & Wang, T. \(2010\). The effects of](#)  
 999 [clouds and aerosols on net ecosystem CO<sub>2</sub> exchange over semi-arid Loess Plateau of Northwest](#)  
 1000 [China. \*Atmospheric Chemistry and Physics\*, 10\(17\), 8205-8218.](#)

1001 Jones, C., McConnell, C., Coleman, K., Cox, P., Falloon, P., Jenkinson, D., & Powlson, D. Global  
 1002 climate change and soil carbon stocks; predictions from two contrasting models for the turnover  
 1003 of organic carbon in soil. *Global Change Biology*, 11(1), 154-166, (2005).

1004 Keppler, F., Hamilton, J. T., Braß, M., & Röckmann, T. Methane emissions from terrestrial plants  
1005 under aerobic conditions. *Nature*, 439(7073), 187-191, (2006).

1006 Kim, H. S., Chung, Y. S., Tans, P. P., & Dlugokencky, E. J. Decadal trends of atmospheric methane  
1007 in East Asia from 1991 to 2013. *Air Quality, Atmosphere & Health*, 8(3), 293-298, (2015).

1008 King, M. D., Kaufman, Y. J., Menzel, W. P., & Tanre, D. Remote sensing of cloud, aerosol, and  
1009 water vapor properties from the Moderate Resolution Imaging Spectrometer (MODIS).  
1010 *Geoscience and Remote Sensing, IEEE Transactions on*, 30(1), 2-27, (1992).

1011 Kirschke, Stefanie., Bousquet, Philippe., Ciais, Philippe., Saunois, Marielle., Canadell, Josep G.,  
1012 Dlugokencky, Edward J., Bergamaschi, Peter., Bergmann, Daniel., Blake, Donald R., Bruhwiler,  
1013 Lori., Cameron-Smith, Philip., Castaldi, Simona., Chevallier, Frédéric., Feng, Liang., Fraser,  
1014 Annemarie., Heimann, Martin., Hodson, Elke L., Houweling, Sander., Josse, Béatrice., Fraser,  
1015 Paul J., Krummel, Paul B., Lamarque, Jean-François., Langenfelds, Ray L., Quéré, Corinne Le.,  
1016 Naik, Vaishali., O'Doherty, Simon., Palmer, Paul I., Pison, Isabelle., Plummer, David., Poulter,  
1017 Benjamin., Prinn, Ronald G., Rigby, Matt., Ringeval, Bruno., Santini, Monia., Schmidt,  
1018 Martina., Shindell, Drew T., Simpson, Isobel J., Spahni, Renato., Steele, L. Paul., Strode, Sarah  
1019 A., Sudo, Kengo., Szopa, Sophie., Werf, Guido R. van der., Voulgarakis, Apostolos., Weele,  
1020 Michiel van., Weiss, Ray F., Williams, Jason E., Guang, Zeng. Three decades of global methane  
1021 sources and sinks, *Nature Geoscience*, volume 6, (2013), doi: 10.1038/NGEO1955.

1022 Koshal. A. K. Spatial temporal climatic change variability of cropping system in western Uttar  
1023 Pradesh, *International Journal of Remote Sensing & Geoscience*, volume 2, issue 3, (2013).

1024 Lewis, A. C., Evans, M. J., Hopkins, J. R., Punjabi, S., Read, K.A., Purvis, R. M., Andrews, S. J.,  
1025 Moller, S. J., Carpenter, L.J., Lee, J. D., Rickard, A. R., Palmer, P. I., and Parrington, M.: The  
1026 influence of biomass burning on the global distribution of selected non-methane organic  
1027 compounds, *Atmos. Chem. Phys.*, 13, 851–867, doi:10.5194/acp-13-851-2013, 2013.

1028 Liu, Yang, Xiufeng Wang, Meng Guo, Hiroshi Tani, Nobuhiro Matsuoka, and Shinji Matsumura.  
1029 "Spatial and temporal relationships among NDVI, climate factors, and land cover changes in  
1030 Northeast Asia from 1982 to 2009." *GIScience & Remote Sensing* 48, no. 3 (2011): 371-393.

1031 Machida, T., K. Kita, Y. Kondo, D. Blake, S. Kawakami, G. Inoue, and T. Ogawa. "Vertical and  
1032 meridional distributions of the atmospheric CO<sub>2</sub> mixing ratio between northern midlatitudes and  
1033 southern subtropics." *Journal of Geophysical Research: Atmospheres* (1984–2012) 107, no. D3  
1034 (2002): BIB-5.

1035 Mahesh, P., N. Sharma, V. K. Dadhwal, P. V. N. Rao, and B. V. Apparao. "Impact of Land-Sea  
1036 Breeze and Rainfall on CO<sub>2</sub> Variations at a Coastal Station. J Earth Sci Clim Change 5: 201. doi:  
1037 10.4172/2157-7617.1000201 Volume 5. Issue 6. (2014).

1038 Mahesh. P, Sreenivas. G, Rao.P.V.N., Dadhwal.V.K.,Sai Krishna. S.V.S. and Mallikarjun. K:  
1039 High precision surface level CO<sub>2</sub> and CH<sub>4</sub> using Off-Axis Integrated Cavity Output Spectroscopy  
1040 (OA-ICOS) over Shadnagar, India, International Journal of Remote Sensing, (2015),  
1041 doi:10.1080/01431161.2015.1104744.

1042 Miller, John B., Luciana V. Gatti, Monica TS d'Amelio, Andrew M. Crotnell, Edward J.  
1043 Dlugokencky, Peter Bakwin, Paulo Artaxo, and Pieter P. Tans. "Airborne measurements indicate  
1044 large methane emissions from the eastern Amazon basin." Geophysical Research Letters 34, no.  
1045 10 (2007).

1046 Monastersky, Richard. "Global carbon dioxide levels near worrisome milestone." Nature 497, no.  
1047 7447 (2013): 13-14.

1048 [Nair, V. S., Moorthy, K. K., Alappattu, D. P., Kunhikrishnan, P. K., George, S., Nair, P. R., &  
1049 Niranjan, K. \(2007\). Wintertime aerosol characteristics over the Indo-Gangetic Plain \(IGP\):  
1050 Impacts of local boundary layer processes and long-range transport. Journal of Geophysical  
1051 Research: Atmospheres \(1984–2012\), 112\(D13\).](#)

1052 Newman, S., Jeong, S., Fischer, M. L., Xu, X., Haman, C. L., Lefer, B., Alvarez, S., Rappenglueck,  
1053 B., Kort, E. A., Andrews, A. E., Peischl, J., Gurney, K. R., Miller, C. E., and Yung, Y. L.: Diurnal  
1054 tracking of anthropogenic CO<sub>2</sub> emissions in the Los Angeles basin megacity during spring, Atmos.  
1055 Chem. Phys., 13, 4359–4372, 2013, doi:10.5194/acp-13-4359-2013.

1056 Nishanth, T., K. M. Praseed, M. K. Satheesh Kumar, and K. T. Valsaraj. "Observational study of  
1057 surface O<sub>3</sub>, NO<sub>x</sub>, CH<sub>4</sub> and total NMHCs at Kannur, India." Aerosol. Air. Qual. Res 14 (2014):  
1058 1074-1088.

1059 Pan, X. L., Kanaya, Y., Wang, Z. F., Liu, Y., Pochanart, P., Akimoto, H., Sun, Y. L., Dong, H. B.,  
1060 Li, J., Irie, H., and Takigawa, M.: Correlation of black carbon aerosol and carbon monoxide in the  
1061 high-altitude environment of Mt. Huang in Eastern China, Atmos. Chem. Phys., 11, 9735-9747,  
1062 doi:10.5194/acp-11-9735-2011, 2011

1063 Paul, J. B., Lapson, L., & Anderson, J. G.. Ultrasensitive absorption spectroscopy with a high-  
1064 finesse optical cavity and off-axis alignment. Applied Optics, 40(27), 4904-4910, (2001).

1065 Patil, M. N., T. Dharmaraj, R. T. Waghmare, T. V. Prabha, and J. R. Kulkarni. "Measurements of  
1066 carbon dioxide and heat fluxes during monsoon-2011 season over rural site of India by eddy  
1067 covariance technique." Journal of Earth System Science 123, no. 1 (2014): 177-185.



1068 Pielke, Roger A., Gregg Marland, Richard A. Betts, Thomas N. Chase, Joseph L. Eastman, John  
1069 O. Niles, and Steven W. Running. "The influence of land-use change and landscape dynamics on  
1070 the climate system: relevance to climate-change policy beyond the radiative effect of greenhouse  
1071 gases." *Philosophical Transactions of the Royal Society of London A: Mathematical, Physical and  
1072 Engineering Sciences* 360, no. 1797 (2002): 1705-1719.

1073 Ramachandran, S., and T. A. Rajesh. "Black carbon aerosol mass concentrations over Ahmedabad,  
1074 an urban location in western India: comparison with urban sites in Asia, Europe, Canada, and the  
1075 United States." *Journal of Geophysical Research: Atmospheres* (1984–2012) 112, no. D6 (2007).  
1076 Salomonson, Vincent V., W. L. Barnes, Peter W. Maymon, Harry E. Montgomery, and Harvey  
1077 Ostrow. "MODIS: Advanced facility instrument for studies of the Earth as a system." *Geoscience  
1078 and Remote Sensing, IEEE Transactions on* 27, no. 2 (1989): 145-153.

1079 Smith, K. A., Ball, T., Conen, F., Dobbie, K. E., Massheder, J., & Rey, A. Exchange of greenhouse  
1080 gases between soil and atmosphere: interactions of soil physical factors and biological processes.  
1081 *European Journal of Soil Science*, 54(4), 779-791, (2003).

1082 Schneising, O., M. Buchwitz, J. P. Burrows, H. Bovensmann, P. Bergamaschi, and W. Peters.  
1083 "Three years of greenhouse gas column-averaged dry air mole fractions retrieved from satellite—  
1084 Part 2: Methane." *Atmos. Chem. Phys* 9, no. 2 (2009): 443-465.

1085 Sharma Neerja, Dadhwal, V.K., Kant, Y., Mahesh, P., Mallikarjun, K., Gadavi, Harish, Sharma,  
1086 Anand., Ali, M.M. Atmospheric CO<sub>2</sub> Variations in Two Contrasting Environmental Sites Over  
1087 India. *Air, Soil and Water Research* 2014:7 61–68, (2014), doi:10.4137/ASWR.S13987.

1088 Sharma, Anu Rani, Shailesh Kumar Kharol, K. V. S. Badarinath, and Darshan Singh. "Impact of  
1089 agriculture crop residue burning on atmospheric aerosol loading—a study over Punjab State,  
1090 India." In *Annales geophysicae: atmospheres, hydrospheres and space sciences*, vol. 28, no. 2, p.  
1091 367. 2010.

1092 Sharma, Neerja, Rabindra K. Nayak, Vinay K. Dadhwal, Yogesh Kant, and Meer M. Ali.  
1093 "Temporal variations of atmospheric CO<sub>2</sub> in Dehradun, India during 2009." *Air, Soil and Water  
1094 Research* 6 (2013): 37.

1095 Stocker, T.F., Qin, D., Plattner, G.K., Alexander, L.V., Allen, S.K., Bindoff, N.L., Bréon, F.M.,  
1096 Church, J.A., Cubasch, U., Emori, S., Forster, P., Friedlingstein, P., Gillett, N., Gregory, J.M.,  
1097 Hartmann, D.L., Jansen, E., Kirtman, B., Knutti, R., Krishna Kumar, K., Lemke, P., Marotzke, J.,  
1098 Masson-Delmotte, V., Meehl, G.A., Mokhov, I.I., Piao, S., Ramaswamy, V., Randall, D., Rhein,  
1099 M., Rojas, M., Sabine, C., Shindell, D., Talley, L.D., Vaughan D.G., and Xie, S.P. Technical  
1100 Summary. In: *Climate Change 2013: The Physical Science Basis. Contribution of Working Group  
1101 I to the Fifth Assessment Report of the Intergovernmental Panel on Climate Change* [Stocker, T.F.,  
1102 D. Qin, G.-K. Plattner, M. Tignor, S.K. Allen, J. Boschung, A. Nauels, Y. Xia, V. Bex and P.M.  
1103 Midgley (eds.)]. Cambridge University Press, Cambridge, United Kingdom and New York, NY,  
1104 USA, (2013).

1105 [Shea, S.J.O, G. Allen<sup>1</sup>, M. W. Gallagher, S. J.-B. Bauguitte, S. M. Illingworth, M. Le Breton, J.](#)  
1106 [B. A. Muller, C. J. Percival, A. T. Archibald, D. E. Oram, M. Parrington\\*, P. I. Palmer, and A. C.](#)  
1107 [Lewis. Airborne observations of trace gases over boreal Canada during BORTAS: campaign](#)  
1108 [climatology, air mass analysis and enhancement ratios. Atmos. Chem. Phys., 13, 12451–12467,](#)  
1109 [2013 atmos-chem-phys.net/13/12451/2013/ doi:10.5194/acp-13-12451-2013](#)

1110 Stohl, Andreas, Markus Hittenberger, and Gerhard Wotawa. "Validation of the Lagrangian particle  
1111 dispersion model FLEXPART against large-scale tracer experiment data." *Atmospheric*  
1112 *Environment* 32, no. 24 (1998): 4245-4264.

1113 [Stull, R. B. \(1988\). Similarity theory. In \*An Introduction to Boundary Layer Meteorology\* \(pp.](#)  
1114 [347-404\). Springer Netherlands.](#)

1116

1117 Taylor J. *An Introduction to Error Analysis: The Study of Uncertainties in Physical Measurement*,  
1118 University Science Books, And ISBN: 093570275X (ISBN13: 9780935702750), (1997).

1119 Thum, T., T. Aalto, T. Laurila, M. Aurela, J. Hatakka, Anders Lindroth, and T. Vesala. "Spring  
1120 initiation and autumn cessation of boreal coniferous forest CO<sub>2</sub> exchange assessed by  
1121 meteorological and biological variables." *Tellus B* 61, no. 5 (2009): 701-717.

1122 Tohjima, Y., Kubo, M., Minejima, C., Mukai, H., Tanimoto, H., Ganshin, A., Maksyutov, S.,  
1123 Katsumata, K., Machida, T., and Kita, K.: Temporal changes in the emissions of CH<sub>4</sub> and CO  
1124 from China estimated from CH<sub>4</sub> / CO<sub>2</sub> and CO / CO<sub>2</sub> correlations observed at Hateruma Island,  
1125 *Atmos. Chem. Phys.*, 14, 1663-1677, doi:10.5194/acp-14-1663-2014, 2014.

1126

1127 Vaghjiani, Ghanshyam L., and A. R. Ravishankara. "New measurement of the rate coefficient for  
1128 the reaction of OH with methane." *Nature* 350, no. 6317 (1991): 406-409.

1129 Wang, B-R., X-Y. Liu, and J-K. Wang. "Assessment of COSMIC radio occultation retrieval  
1130 product using global radiosonde data." *Atmospheric Measurement Techniques* 6, no. 4 (2013):  
1131 1073-1083.

1132 [Wang, G., J. Huang\\*, W. Guo, J. Zuo, J. Wang, J. Bi, Z. Huang, and J. Shi, 2010: Observation](#)  
1133 [analysis of land-atmosphere interactions over the Loess Plateau of northwest China, J. Geophys.](#)  
1134 [Res., 115, D00K17, doi:10.1029/2009JD013372.](#)

1135 Worthy, Douglas EJ, Elton Chan, Misa Ishizawa, Douglas Chan, Christian Poss, Edward J.  
1136 Dlugokencky, Shamil Maksyutov, and Ingeborg Levin. "Decreasing anthropogenic methane  
1137 emissions in Europe and Siberia inferred from continuous carbon dioxide and methane  
1138 observations at Alert, Canada." *Journal of Geophysical Research: Atmospheres* (1984–2012) 114,  
1139 no. D10 (2009).

1140  
1141

1142 Yunck, Thomas P., Liu Chao-Han, and Randolph Ware. "A history of GPS sounding." Terrestrial  
1143 Atmospheric and Oceanic Sciences 11, no. 1 (2000): 1-20.

1144

1145

1146

1147

1148

1149

1150

1151

1152

1153

1154 **Table 1** Data used

1155

1156

1157

1158

1159

1160

1161

1162

1163

1164

1165

1166

1167  
1168  
1169

Sensor	Period	Parameter	resolution	Source
GGA-24EP	Jan-2014 to Dec 2014	CO <sub>2</sub> ,CH <sub>4</sub> and H <sub>2</sub> O	1 Hz time	ASL,NRSC
42i-NO-NO <sub>2</sub> -NO <sub>x</sub>	Jul-2014 to Sep-2014	NO <sub>x</sub> (=NO+N O <sub>2</sub> )	1 min time	ASL,NRSC
49i-O <sub>3</sub>	Jul-2014 to Sep-2014	O <sub>3</sub>	1 min time	ASL,NRSC
AWS	Jan-2014 to Dec-2014	WS,WD,AT,RH	60 min time	NRSC
Terra/MODIS	Jan-2014 to Dec-2014	NDVI	5 Km horizontal	<a href="http://ladsweb.nascom.nasa.gov/data/search.html">http://ladsweb.nascom.nasa.gov/data/search.html</a>
COSMIC-IDVAR	Jul-2013 to Jun-2014	Refractivity (N)	0.1 Km vertical	
HYSPLIT	Jan-2014 to Dec-2014	Backward trajectory	5 day isentropic model (1km to 4 km)	<a href="http://ww.arl.noaa.gov/ready/hysplit4.html">http://ww.arl.noaa.gov/ready/hysplit4.html</a>
FEER v1	Jan-2013 to Dec-2013	fire radiative power (FRP)		<a href="http://ladsweb.nascom.nasa.gov/data/search.html">http://ladsweb.nascom.nasa.gov/data/search.html</a>

1170  
1171  
1172  
1173  
1174  
1175  
1176  
1177  
1178  
1179  
1180  
1181

**Table 2** Statistical correlation between CO<sub>2</sub> and CH<sub>4</sub>

<u>S.No</u>	<u>Seasons</u>	<u>Correlation coefficient (R)</u>	<u>Slope</u> $\left(\frac{Y_{CH_4} (ppm)}{X_{CO_2} (ppm)}\right)$	<u><math>\Psi_{slope}</math></u> <u>(ppm)</u>	<u><math>\Psi_{v-int}</math></u> <u>(ppm)</u>
<u>1</u>	<u>Monsoon (JJAS)</u>	<u>0.61</u>	<u>0.005</u>	<u>0.00015</u>	<u>1.91</u>
<u>2</u>	<u>Post-monsoon (OND)</u>	<u>0.72</u>	<u>0.0065</u>	<u>0.00014</u>	<u>1.52</u>
<u>3</u>	<u>Winter (JF)</u>	<u>0.80</u>	<u>0.0085</u>	<u>0.00018</u>	<u>9.13</u>
<u>4</u>	<u>Pre-monsoon (MAM)</u>	<u>0.80</u>	<u>0.0059</u>	<u>0.00021</u>	<u>2.73</u>

**Table 23** Seasonal amplitudes of CO<sub>2</sub> and CH<sub>4</sub> over study region arriving from different directions

Wind Direction	Winter $\frac{CO_2}{CH_4}$ (ppm)	Pre-monsoon $\frac{CO_2}{CH_4}$ (ppm)	Monsoon $\frac{CO_2}{CH_4}$ (ppm)	Post-monsoon $\frac{CO_2}{CH_4}$ (ppm)
0-45	399.85/1.98	410.37/1.94	400.72/1.91	395.13/2.02
45-90	391.66/1.94	399.59/1.89	388.82/1.91	390.23/1.98
90-135	391.57/1.93	397.79/1.87	388.99/1.87	389.06/1.97
135-180	389.34/1.89	393.87/1.85	391.81/1.86	387.69/1.97
180-225	391.14/1.89	396.75/1.85	390.28/1.82	392.30/2.02
225-270	389.13/1.88	394.81/1.86	390.26/1.82	384.40/1.94
270-315	388.68/1.87	398.68/1.89	389.58/1.82	384.99/1.93
315-360	390.87/1.91	401.17/1.89	387.58/1.83	389.32/1.98

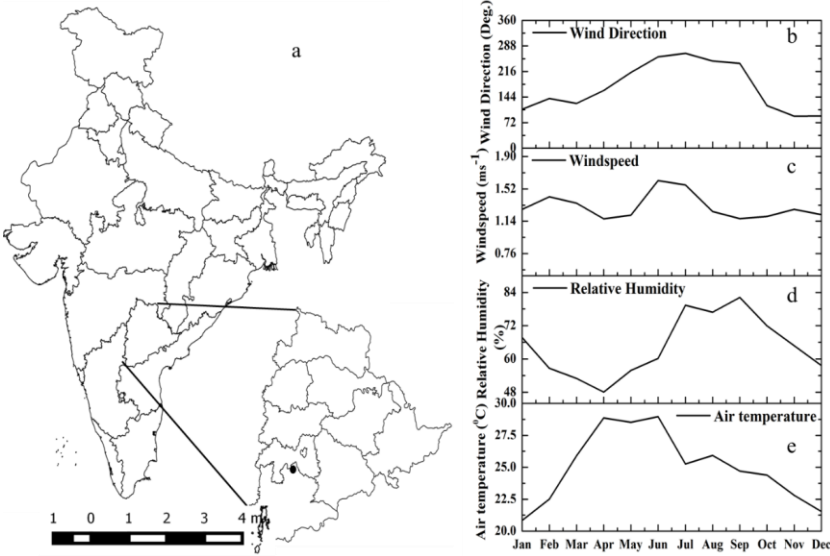
**Table 3** Statistical correlation between CO<sub>2</sub> and CH<sub>4</sub>

1203  
1204  
1205  
1206  
1207  
1208  
1209  
1210  
1211  
1212  
1213  
1214  
1215  
1216  
1217  
1218  
1219  
1220  
1221  
1222  
1223  
1224  
1225  
1226  
1227  
1228  
1229  
1230

S.No	Seasons	Correlation coefficient (R <sup>2</sup> )	Slope $\frac{y_{CH4}(ppm)}{x_{CO2}(ppm)}$	$\Psi_{slope}$ (ppm)	$\Psi_{\gamma-int}$ (ppm)
1	Monsoon (JJAS)	0.6137	0.005	0.00015	1.91
2	Post-monsoon (OND)	0.7252	0.0065	0.00014	1.52
3	Winter (JF)	0.8061	0.0085	0.00018	9.13
4	Pre-monsoon (MAM)	0.8064	0.0059	0.00021	2.73

**Table 4** Cluster analysis of air mass trajectories reaching Shadnagar at various heights during different seasons

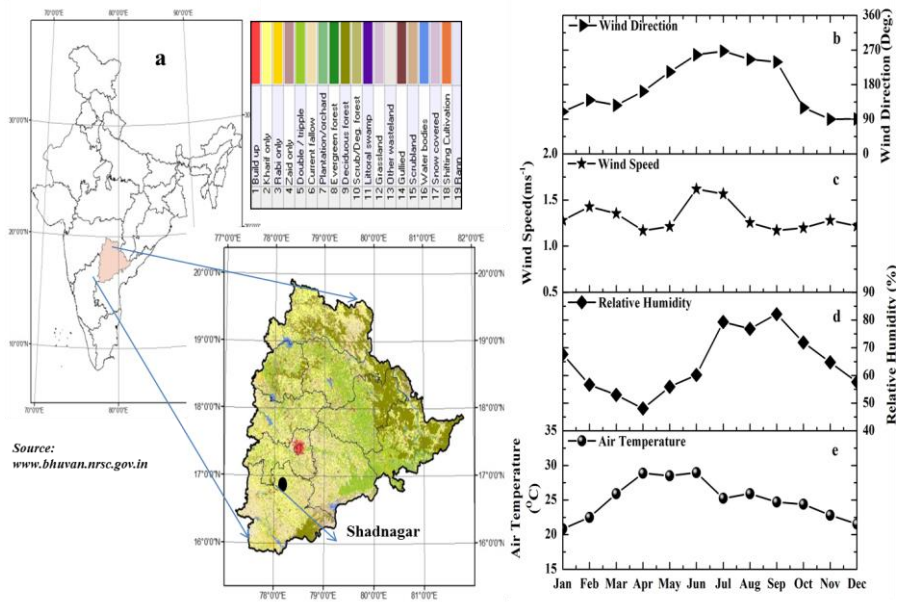
Seasonal Backward trajectory (%)	NW				NE				SE				SW			
	1 km	2 km	3 km	4 km	1 km	2 km	3 km	4 km	1 km	2 km	3 km	4 km	1 km	2 km	3 km	4 km
Winter	54	32	2	0	32	24	44	52	10	25	11	7	4	19	42	41
Pre-monsoon	24	9	8	1	26	31	64	78	36	46	2	10	14	14	26	11
Monsoon	0	1	7	19	12	34	80	70	4	4	4	6	84	61	9	5
Post-monsoon	42	15	11	14	47	53	41	49	8	30	32	26	3	2	16	11



Formatted: Font: (Default) Times New Roman, 12 pt

1253  
1254

Formatted: Font: (Default) Times New Roman, Bold



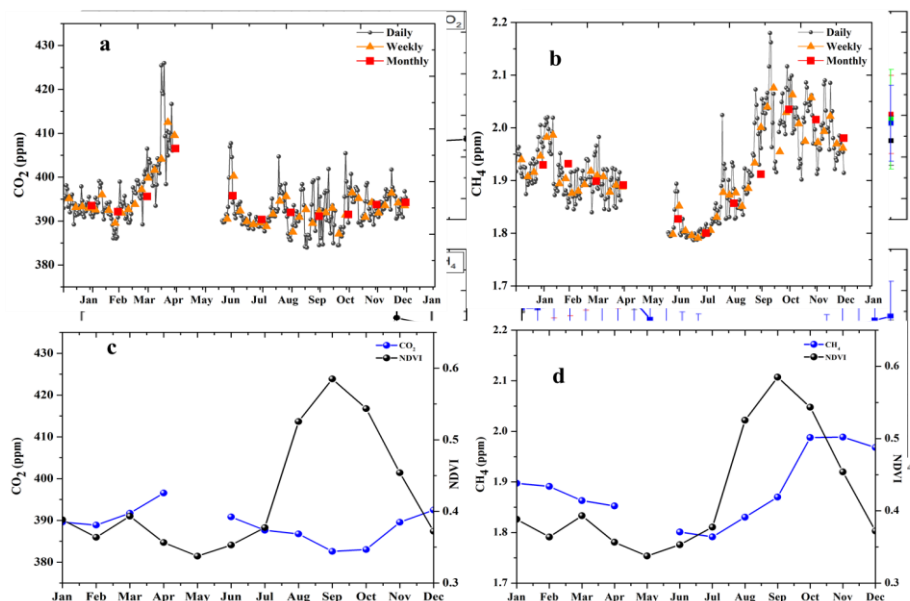
1255  
1256  
1257  
1258  
1259  
1260

**Figure 1** a) Schematic representation of study area; b-e) Seasonal variation of prevailing meteorological conditions during 2014 study period



1261

Formatted: Font: (Default) Times New Roman, Bold



1262

Formatted: Font: (Default) Times New Roman, Bold

1263

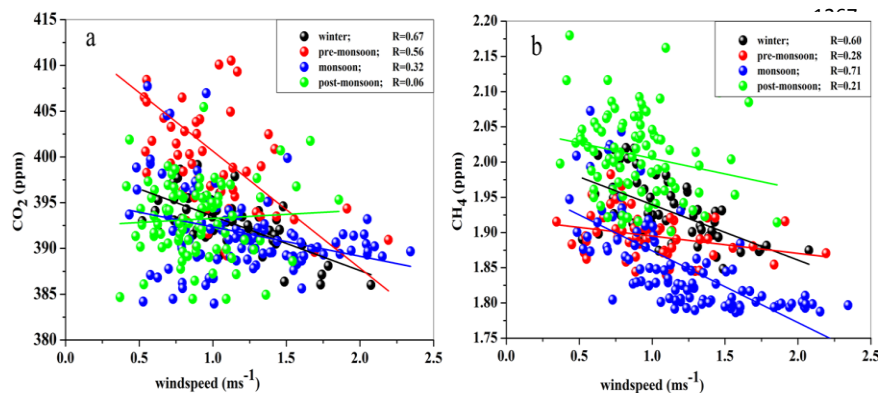
1264

1265

**Figure 2** a-b) Temporal Seasonal variations of CO<sub>2</sub> and CH<sub>4</sub>; c-d) Seasonal variations of CO<sub>2</sub> and CH<sub>4</sub> in conjunction with NDVI (Normalized Difference Vegetation Index) diurnal variations of CO<sub>2</sub> and CH<sub>4</sub> during 2014

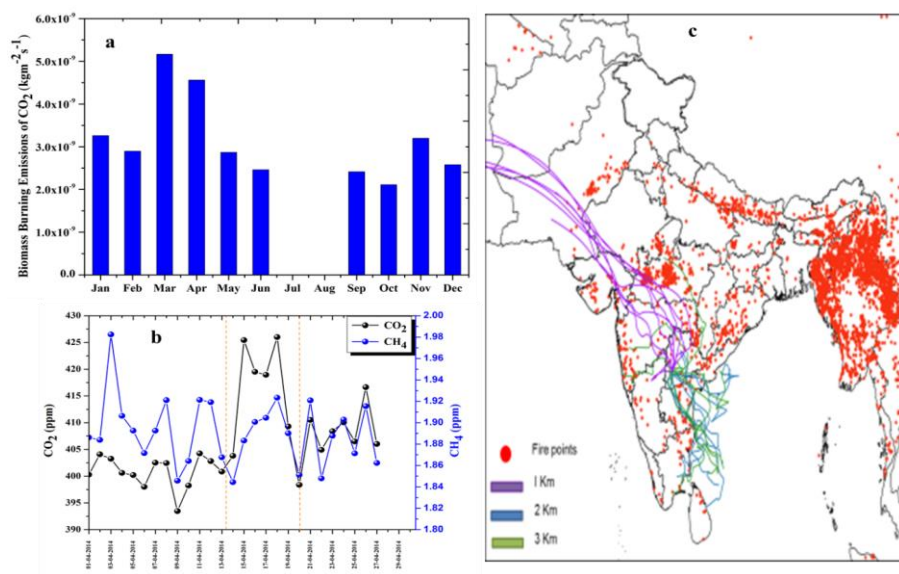
Formatted: Subscript

1266



1276

1277  
1278



1279

Formatted: Font: (Default) Times New Roman, Bold

1280  
1281

1282 **Figure 3** a) Long term analysis of CO<sub>2</sub> biomass burning emissions over study region b) Biomass  
1283 signatures on CO<sub>2</sub>/CH<sub>4</sub> during 14-21 April 2014, a case study c) Spatial distribution of MODIS derived fire  
1284 counts over Indian region during 14-21 April 2014. Scatterplot between wind speed and GHG's (CO<sub>2</sub> and  
1285 CH<sub>4</sub>).

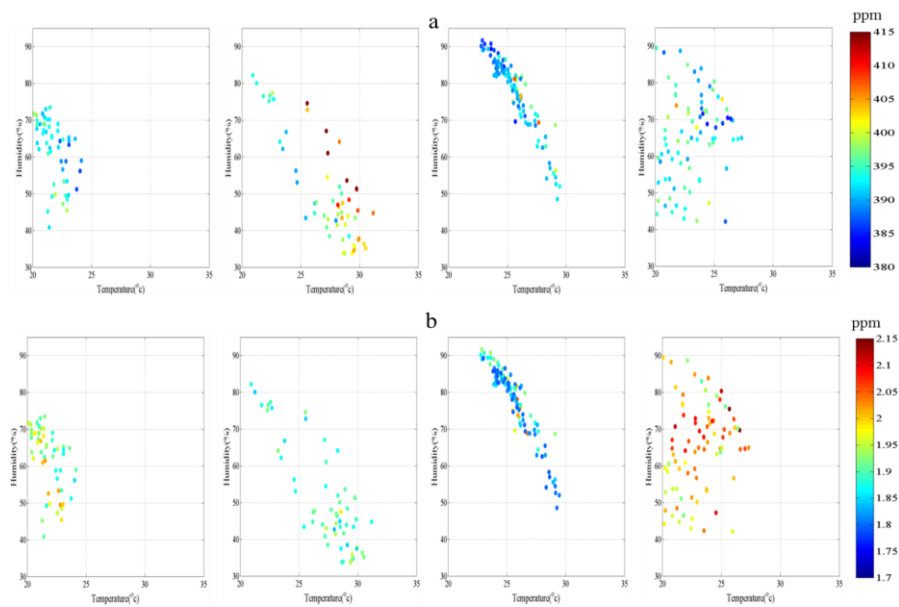
Formatted: Subscript

Formatted: Subscript

Formatted: Font: 11 pt

1286

Formatted: Font: (Default) Times New Roman



1287

1288

1289

1290

1291

1292

1293

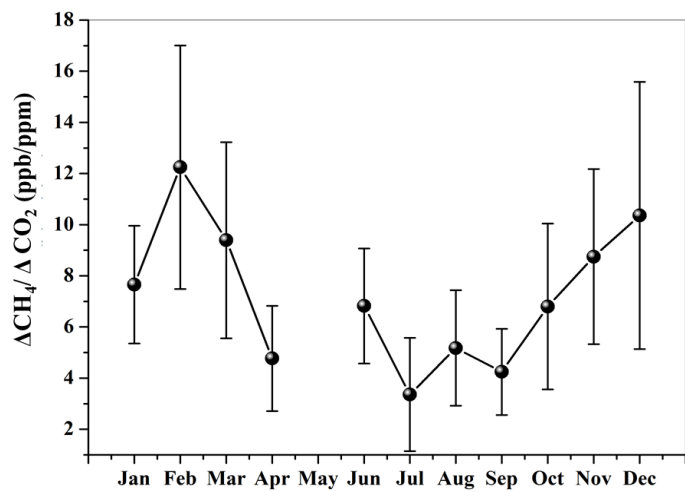
1294

1295

1296

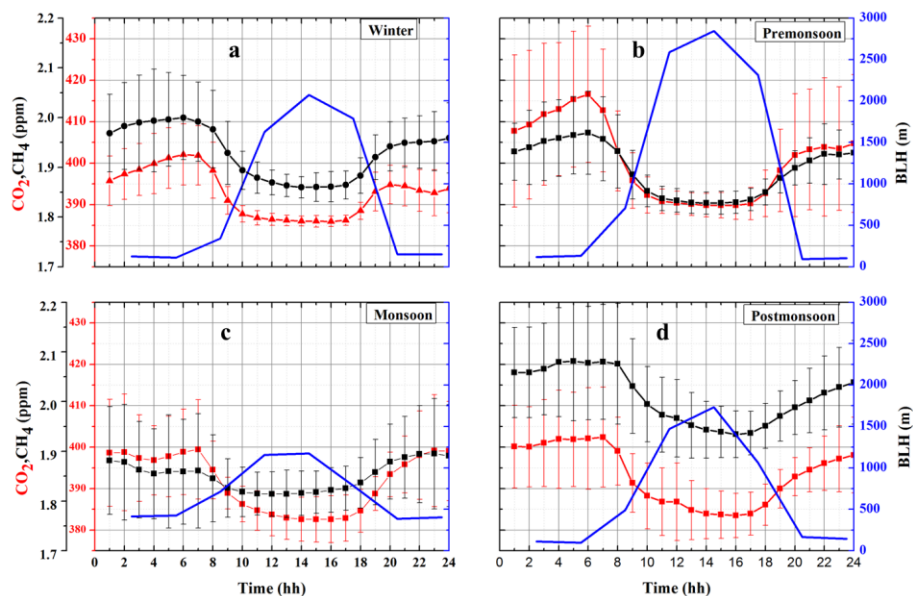
1297

1298



1299 **Figure 4** Monthly variation of  $\Delta\text{CH}_4/\Delta\text{CO}_2$  during study period

Formatted: Font: (Default) Times New Roman

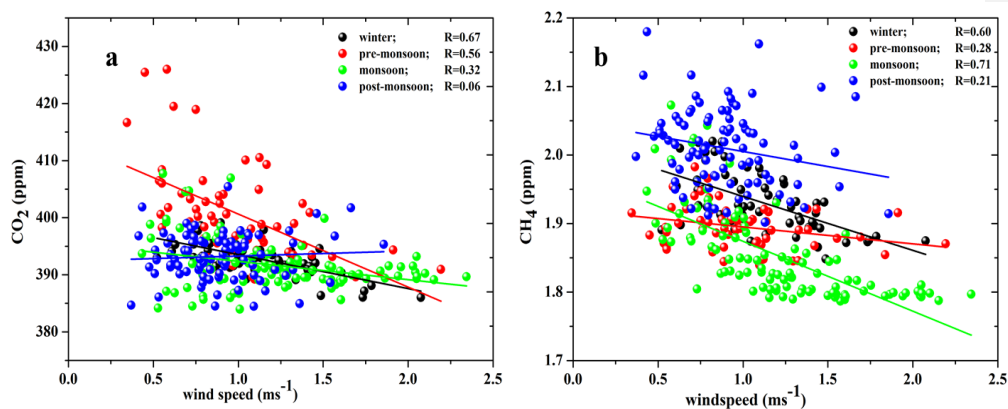


1300 **Figure 5 a-d)** Seasonal variations of diurnal averaged  $\text{CO}_2/\text{CH}_4$  against boundary layer height during 2014

Formatted: Subscript

Formatted: Subscript

Formatted: Font: (Default) Times New Roman



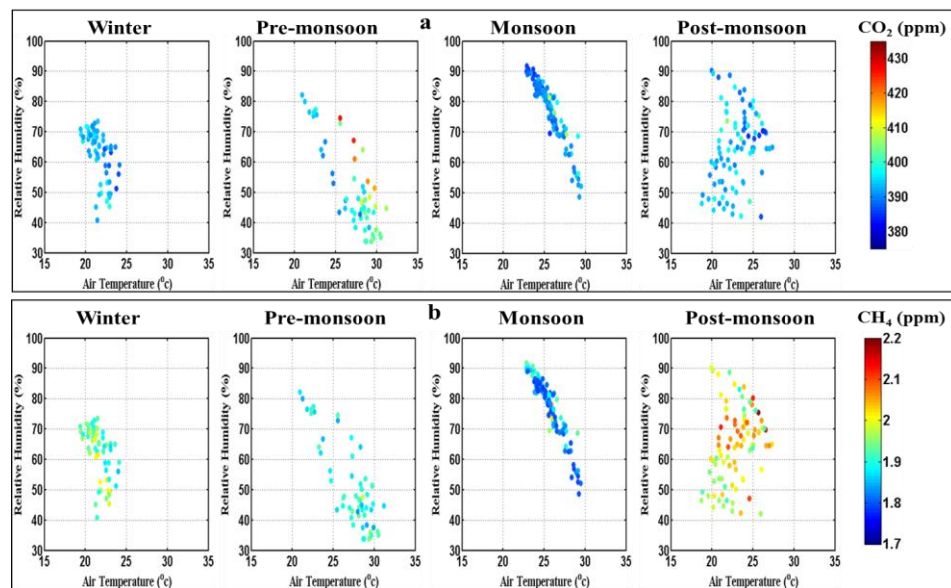
1303

Formatted: Left

1304

Figure 6 a-b) Daily mean scatterplot between wind speed and GHGs ( $\text{CO}_2$  and  $\text{CH}_4$ ).

Formatted: Font: (Default) Times New Roman



1305

Figure 7 a-b) Daily mean seasonal variation of  $\text{CO}_2$  and  $\text{CH}_4$  as function of humidity and air temperature during 2014

Formatted: Subscript

1306

1307

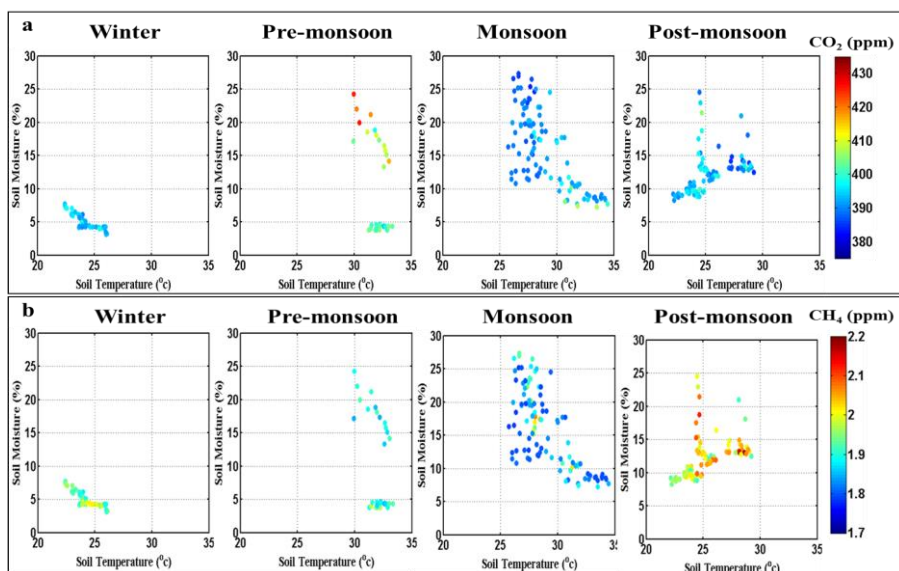
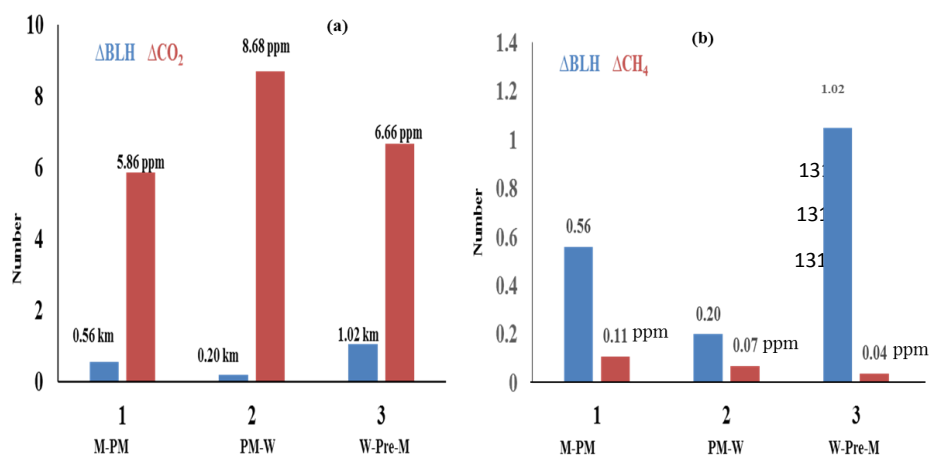
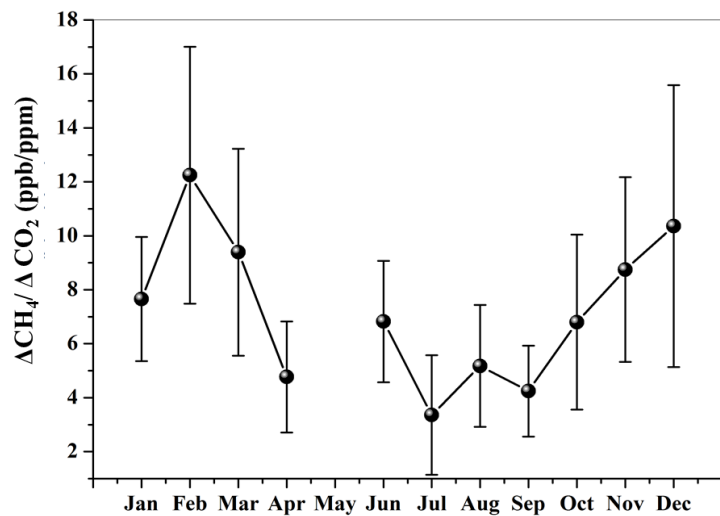


Figure 8 a-b) Daily mean seasonal variation of CO<sub>2</sub> and CH<sub>4</sub> as function of soil temperature and soil moisture during 2014 a) Seasonal variation of CO<sub>2</sub> as function of humidity and temperature during winter, pre-monsoon, monsoon and post-monsoon. b) Seasonal variation of CH<sub>4</sub> as function of humidity and temperature during respective seasons

Formatted: Font: (Default) Times New Roman

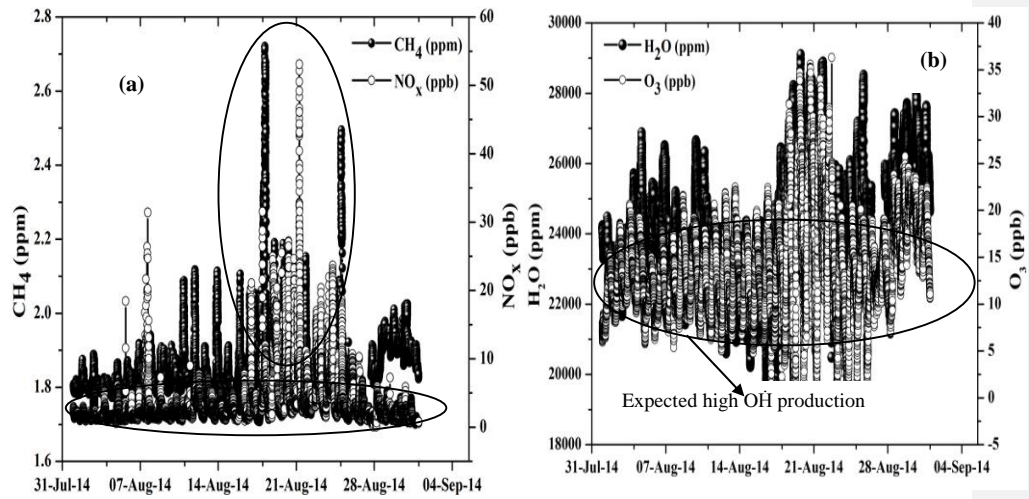


**Figure 59** Seasonal difference in BLH variations of against respective change in -a) CO<sub>2</sub> and b) CH<sub>4</sub> against boundary layer height change



**Figure 6** Monthly variation of ΔCH<sub>4</sub>/ΔCO<sub>2</sub> during study period

1339



1340

1341

1342

1343 **Figure 7** Time series analysis of a)  $\text{CH}_4$  vs.  $\text{NO}_x$ , b)  $\text{H}_2\text{O}$  vs.  $\text{O}_3$

1344

1345

1346

1347

1348

1349

1350

1351

1352

1353

1354

1355

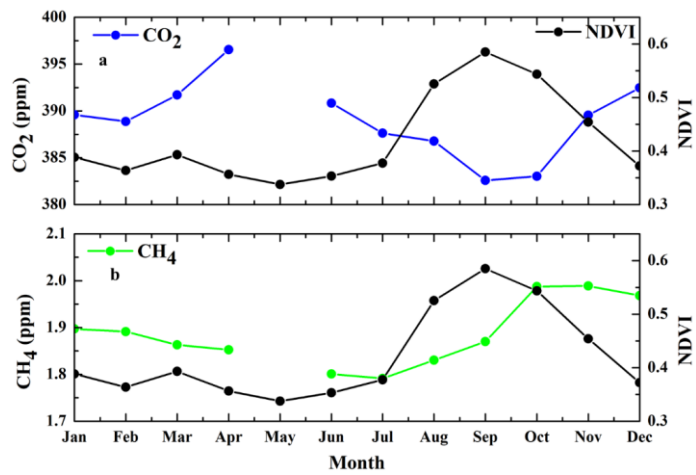




**Figure 8** a) Seasonal variation of CO<sub>2</sub> in conjunction with NDVI (Normalized Difference Vegetation Index). b) Seasonal variation of CH<sub>4</sub> in conjunction with NDVI

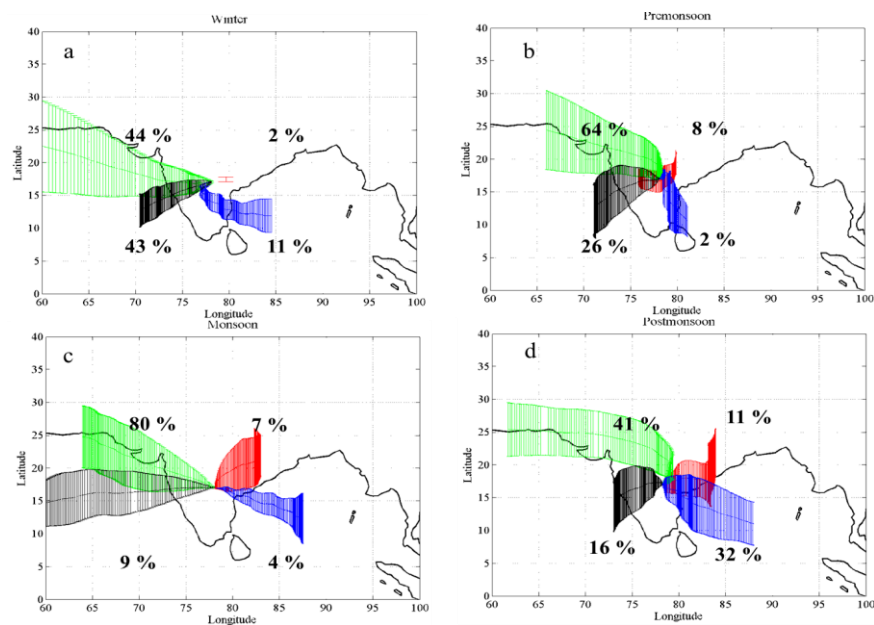


**Figure 9** a-d) Long range circulation of air mass trajectories ending over Shadnagar at 3 km during winter, pre-monsoon, monsoon and post-monsoon

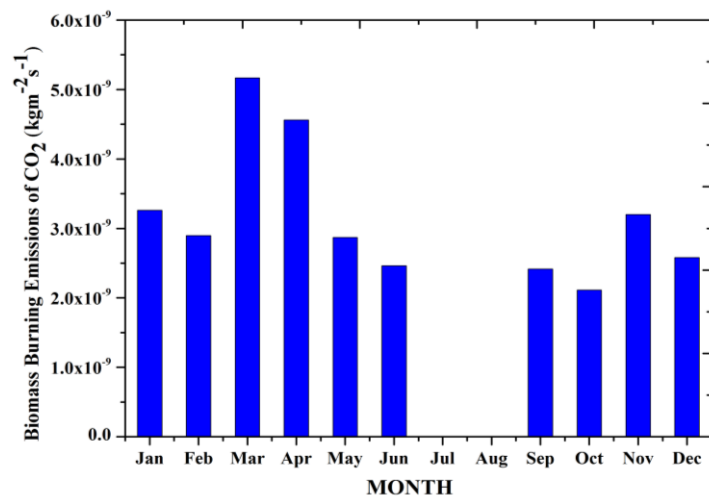


**Figure 10** Long term analysis of CO<sub>2</sub> biomass burning emissions over study region